Longitudinal Spin Structure of the Proton in RG-C

Derek Holmberg

6-23-26

WILLIAM & MARY

CHARTERED 1693

The Proton Spin Structure

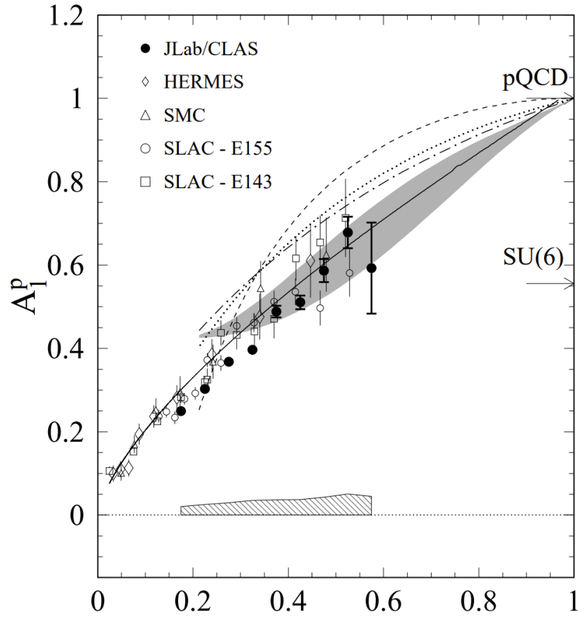

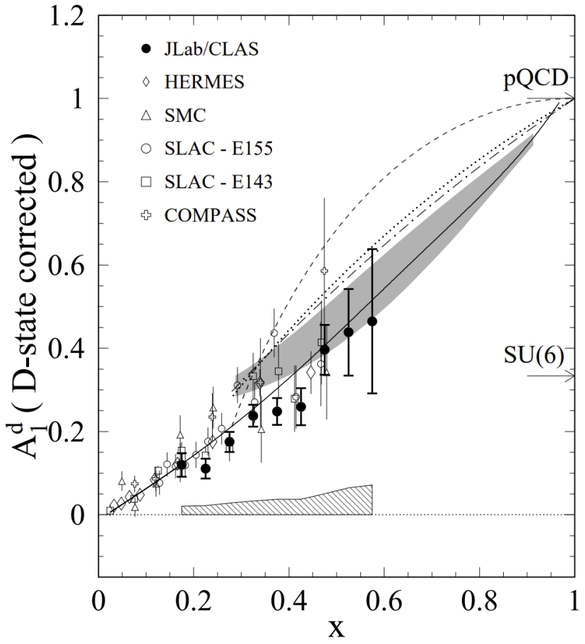

The Longitudinal Spin Structure of the Nucleon:
A 12 GeV Research Proposal to Jefferson Lab (PAC 30) [Ref. 1]

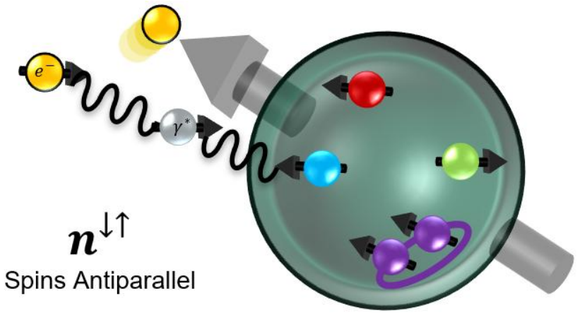

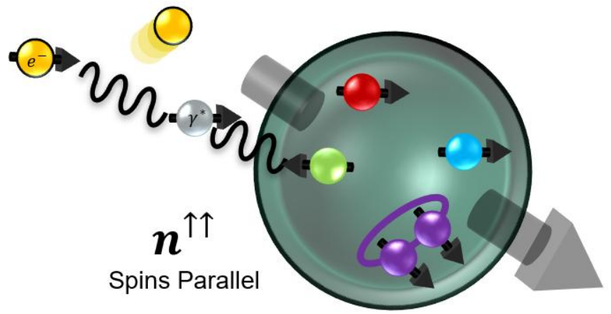

- One goal of Run Group C is measuring the proton/deuteron longitudinal spin structure at large x
- Not much precise data above $x = 0.5$, leaving open possibilities of quark behavior
- Probed via polarized ep or ed DIS scattering and measuring electron double spin asymmetry $A_{||}$

$$A_{||}(x,Q^2) = \frac{n^{\downarrow\uparrow} - n^{\uparrow\uparrow}}{n^{\downarrow\uparrow} + n^{\uparrow\uparrow}} \propto D\left(A_1(x,Q^2) + \eta A_2(x,Q^2)\right)$$

A_1, A_2 = Virtual Photon Asymmetries

$$A_1(x,Q^2) = \frac{g_1 + \gamma^2 g_2}{F_1} \approx \frac{g_1}{F_1} = \frac{\sum_i e_i^2 \Delta q_i(x,Q^2)}{\sum_i e_i^2 q_i(x,Q^2)}$$

- Measurement of A_1 allows us to evaluate proton spin structure models and calculate moments, sum rules, PDFs

Run Group C Experimental Setup

- Ran from June 2022 to March 2023 for 80 PAC days (120 scheduled)
- RG-C data divided into five run periods:

Run Period	Run Range	Torus Configuration	Solenoid Configuration	Inbending or Outbending
Summer 2022	16128 – 16772	Negative	Negative	Inbending
Fall 2022 (Neg.)	16859 – 17183	Negative	Negative	Inbending
Fall 2022 (Pos.)	17188 – 17408	Negative	Positive	Inbending
Spring 2023 (Inb.)	17482 – 17768	Negative	Negative	Inbending
Spring 2023 (Outb.)	17769 – 17811	Positive	Negative	Outbending

- DIS electrons detected in the Forward Detector

- Polarized protons/deuterons from the Run Group C Polarized Target:
  - Ammonia crystals, polarized via dynamic nuclear polarization (DNP)
  - Cool to ~1 K in a 5 T field generated by solenoid, where free electrons almost completely polarize
  - Using microwaves with a frequency of $\nu_{ESR} \pm \nu_{NMR}$ (~140 GHz), transfer electron polarization to the protons (or deuterons)
  - ~85% for protons, ~25% for deuterons

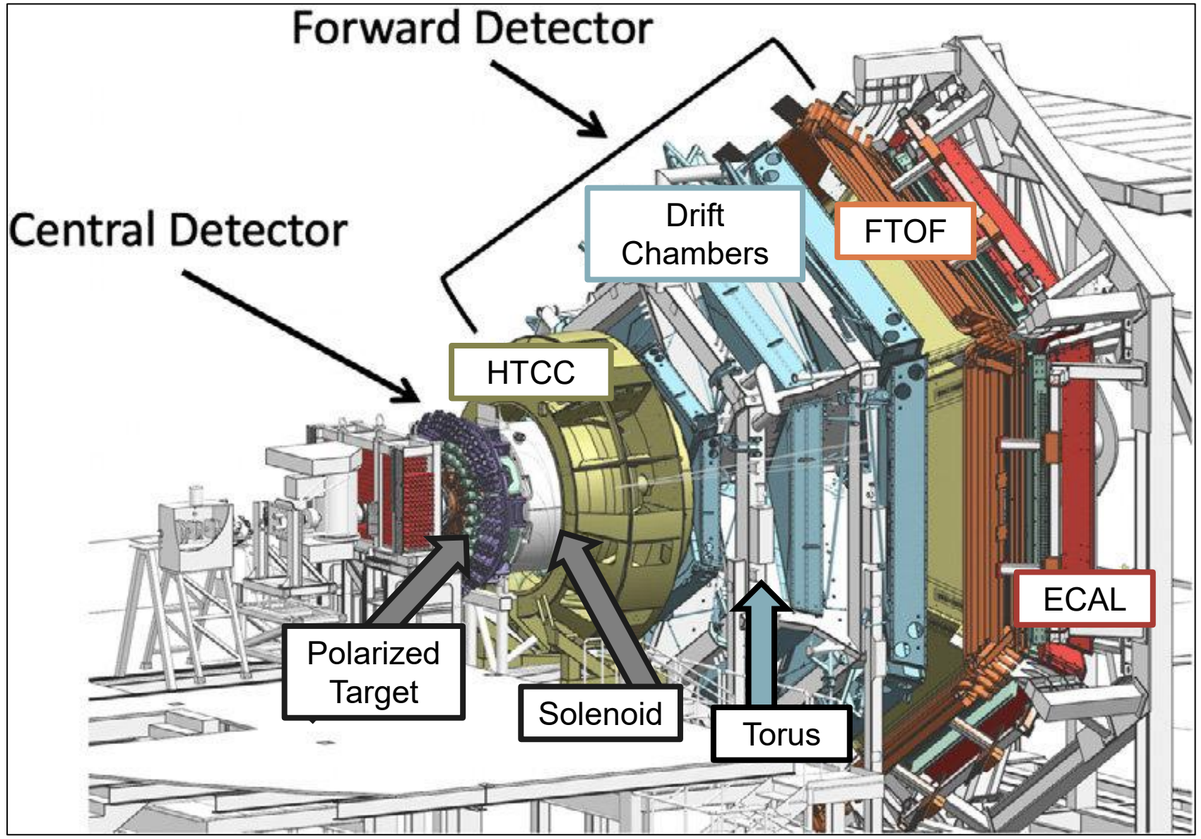

Diagram of CLAS12 Detector, Ziegler et. al. [Ref. 2]

Run Group C Experimental Setup

- Ran from June 2022 to March 2023 for 80 PAC days (120 scheduled)
- RG-C data divided into five run periods:

Run Period	Run Range	Torus Configuration	Solenoid Configuration	Inbending or Outbending
Summer 2022	16128 – 16772	Negative	Negative	Inbending
Fall 2022 (Neg.)	16859 – 17183	Negative	Negative	Inbending
Fall 2022 (Pos.)	17188 – 17408	Negative	Positive	Inbending
Spring 2023 (Inb.)	17482 – 17768	Negative	Negative	Inbending
Spring 2023 (Outb.)	17769 – 17811	Positive	Negative	Outbending

- DIS electrons detected in the Forward Detector

- Polarized protons/deuterons from the Run Group C Polarized Target:
  - Ammonia crystals, polarized via dynamic nuclear polarization (DNP)
  - Cool to ~1 K in a 5 T field generated by solenoid, where free electrons almost completely polarize
  - Using microwaves with a frequency of $\nu_{ESR} \pm \nu_{NMR}$ (~140 GHz), transfer electron polarization to the protons (or deuterons)
  - ~85% for protons, ~25% for deuterons

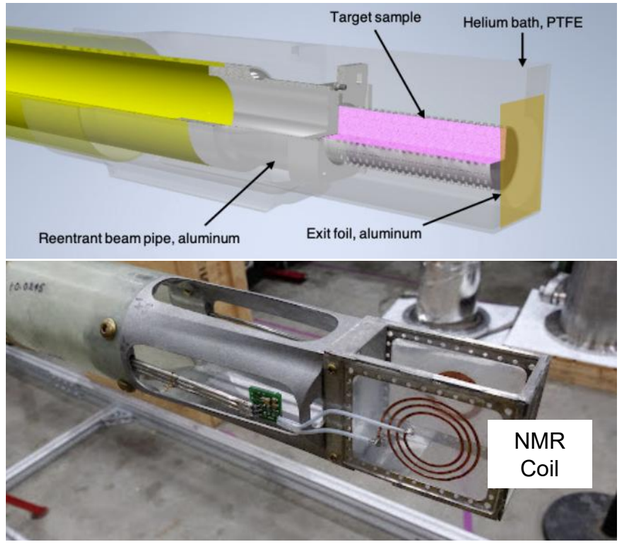

Pictures taken from C. Keith et. al. [Ref.3]

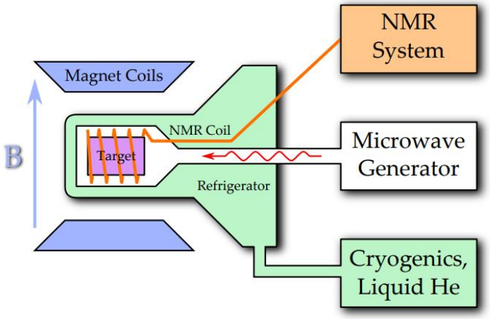

Cell diagram taken from J. Maxwell [Ref.4]

Ammonia crystals unexposed to beam (left), crystals after beam exposure (right). Purple color from paramagnetic centers.

Unpolarized Background

- Unpolarized background: N, Al, He nuclei in target/bath
- Reduces measured $A_{||}$, and cannot be removed with vertex/kinematic cuts
- Quantified using a dilution factor D_F

$$D_F = \frac{Y_H}{Y_{Ammonia}} = \frac{3\sigma_H \ell_A \rho_A}{(3\sigma_H + \sigma_N)\ell_A \rho_A + \sigma_{He}\ell_{He}\rho_{He} + \sigma_{Al}\ell_{Al}\rho_{Al}}$$

- $D_F \equiv$ ratio of the yield from hydrogen to the yield from all target cell material

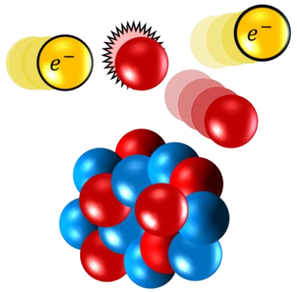

Ideal ep Scattering

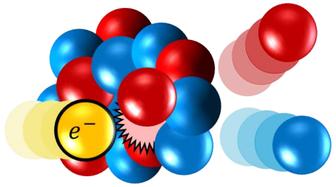

N, Al Nuclei Scattering

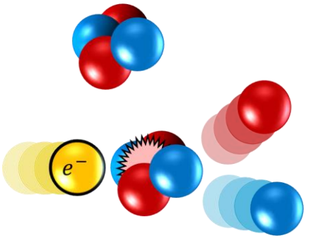

Liquid He Scattering

- Must also account for polarization of beam electrons and target particles: $P_b P_t$
- Dividing $A_{||}$ by D_F and $P_b P_t$ accounts for the background

$$A_{||,phys} = \frac{A_{||,raw}}{D_F P_b P_t} \propto D(A_1 + \eta A_2)$$

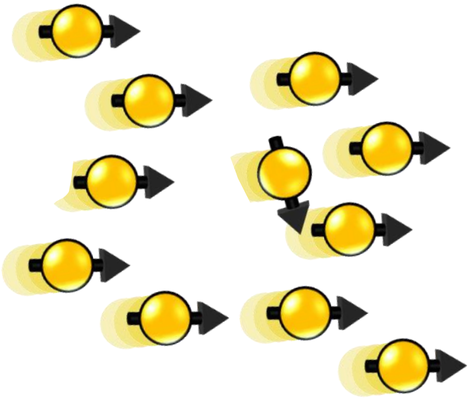

Polarized beam electrons

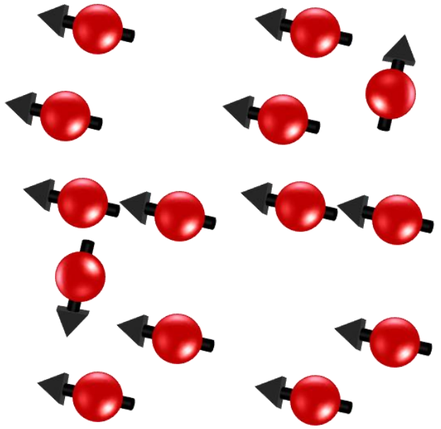

Polarized target protons

Calculating the Dilution Factor

- Advantageous to write D_F in terms of scattering counts from background targets instead of cross sections
- Counts from the targets are functions of the cross sections
- Using information from all targets, write the yields in terms of scattering counts
- $n_A(\sigma_{Al}, \sigma_{He}, \sigma_C, \sigma_H)$, where $\frac{7}{6}\sigma_C \approx \sigma_N$
- $n_{MT}(\sigma_{Al}, \sigma_{He})$, $n_C(\sigma_{Al}, \sigma_{He}, \sigma_C)$
- $n_{CH}(\sigma_{Al}, \sigma_{He}, \sigma_C, \sigma_H)$, $n_F(\sigma_{Al})$

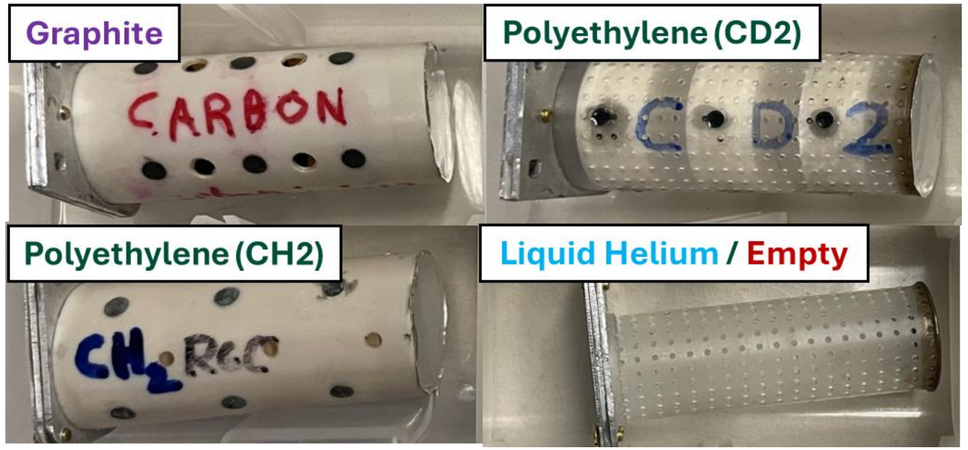

- Solving for the yields and rewriting the D_F:

$$D_F(x, Q^2) = \frac{(n_A - n_{MT})(n_{CH} + An_C + Bn_{MT} + Cn_F)}{n_A(n_{CH} + Dn_C + En_{MT} + Fn_F)}$$

- Packing fraction P_F is the target volume fraction occupied by the ammonia crystals

$$P_F(x, Q^2) = \frac{G(n_A - n_{MT})}{n_{CH} + Dn_C + En_{MT} + Fn_F}$$

$A \ldots G \propto \ell_i, \rho_i$ of target materials

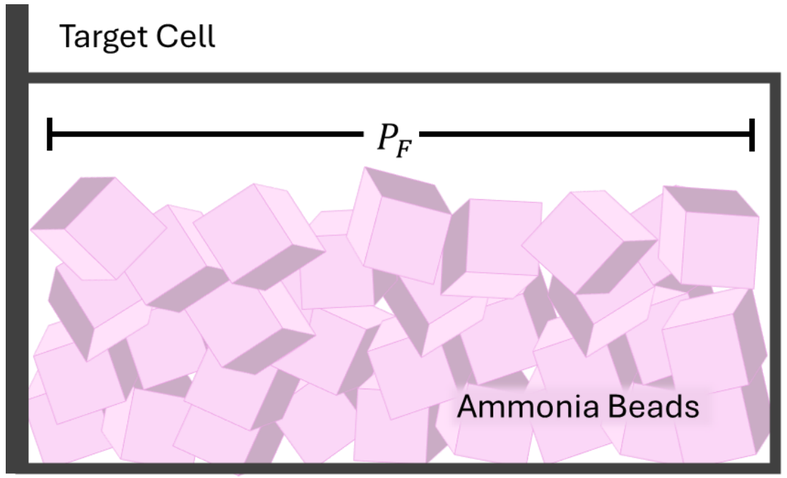

Electron PID Cuts

- Inclusive DIS electrons: $ep \rightarrow eX,\ ed \rightarrow eX$
- Event Builder PID cuts:
  - Trigger electrons in the Forward Detector
  - > 60 MeV energy in PCAL, > 2 photoelectrons in HTCC, broad sampling fraction cut
- Kinematic (DIS) cuts:
  - E' > 2.6 GeV, $7° < \theta < 40°$, $Q^2 > 2.2\ \mathrm{GeV}^2$, $W > 2\ \mathrm{GeV}$
  - -9 cm $\leq V_Z \leq$ 1 cm (Summer), -7.5 cm $\leq V_Z \leq$ 2.5 cm for all other run periods
- QADB cuts
- Fiducial cuts:
  - Drift chamber edge cuts: edge ≡ distance to *any* edge of detector
  - Based on average value of track quality χ^2_{track} versus distance to edge
  - EdgeR1 > 4 cm, EdgeR2 > 5 cm, Edge R3 > 8 cm
  - ECAL edge cuts based on scintillator strip position lv, lw where sampling fraction (SF) dips below 0.2
  - $SF = (E_{PCAL} + E_{ECIN} + E_{COUT})/P,\ SF \approx 0.24$ for electrons
  - $lv, lw > 13.5$ cm for sectors 2-6, $lv, lw > 22.5$ cm for sector 1 (above run 16156)
  - Sector-dependent sampling fraction cuts developed by Timothy Hayward

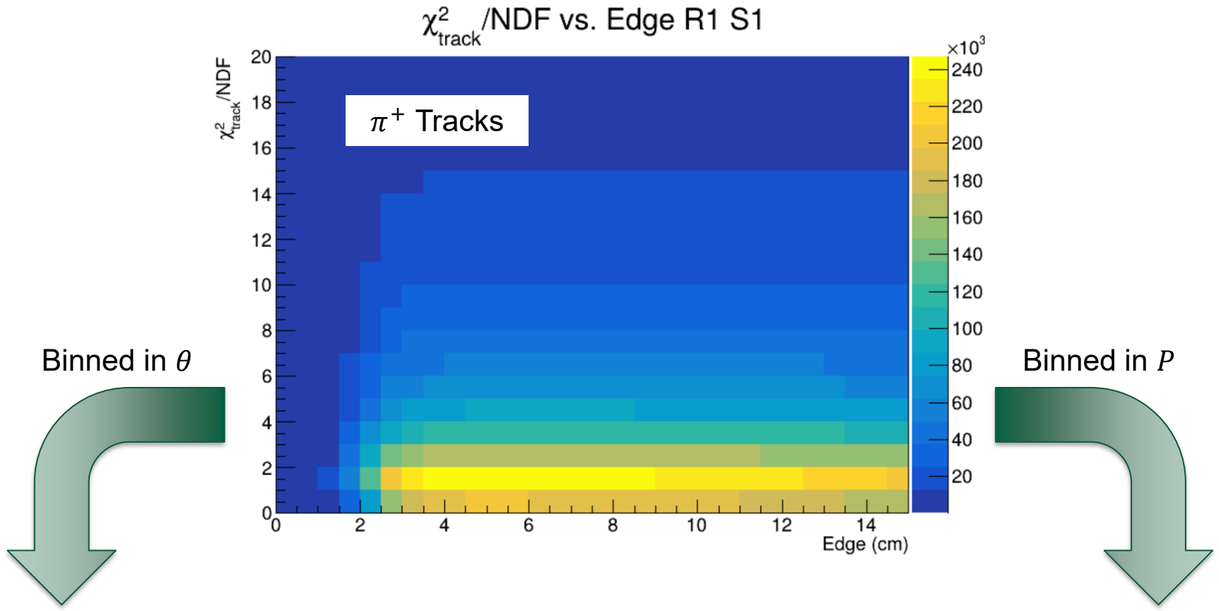

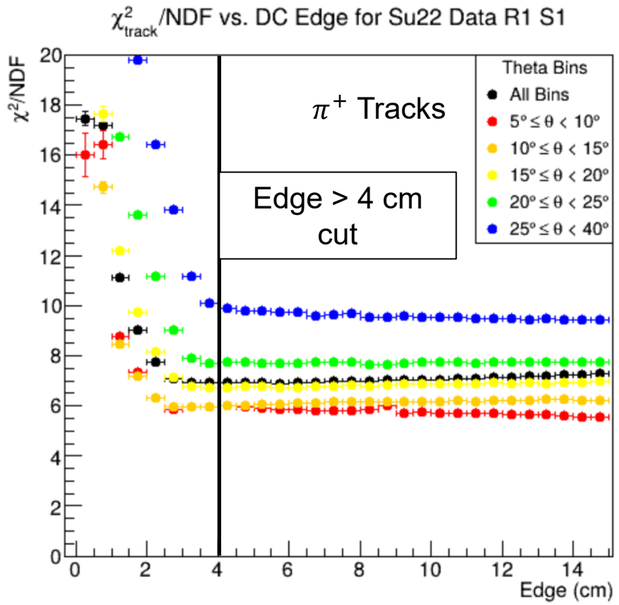

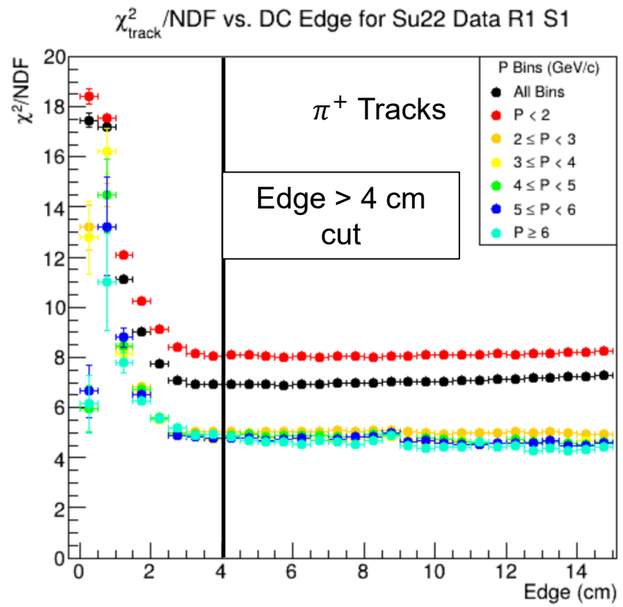

Electron PID Cuts

- Inclusive DIS electrons: $ep \rightarrow eX,\ ed \rightarrow eX$
- Event Builder PID cuts:
  - Trigger electrons in the Forward Detector
  - > 60 MeV energy in PCAL, > 2 photoelectrons in HTCC, broad sampling fraction cut
- Kinematic (DIS) cuts:
  - E' > 2.6 GeV, $7° < \theta < 40°$, $Q^2 > 2.2\ \mathrm{GeV}^2$, $W > 2\ \mathrm{GeV}$
  - -9 cm $\leq V_Z \leq$ 1 cm (Summer), -7.5 cm $\leq V_Z \leq$ 2.5 cm for all other run periods
- QADB cuts
- Fiducial cuts:
  - Drift chamber edge cuts: edge ≡ distance to *any* edge of detector
  - Based on average value of track quality χ^2_{track} versus distance to edge
  - EdgeR1 > 4 cm, EdgeR2 > 5 cm, Edge R3 > 8 cm
  - ECAL edge cuts based on scintillator strip position lv, lw where sampling fraction (SF) dips below 0.2
  - $SF = (E_{PCAL} + E_{ECIN} + E_{COUT})/P,\ SF \approx 0.24$ for electrons
  - $lv, lw > 13.5$ cm for sectors 2-6, $lv, lw > 22.5$ cm for sector 1 (above run 16156)
  - Sector-dependent sampling fraction cuts developed by Timothy Hayward

Fit each L-bin to a gaussian

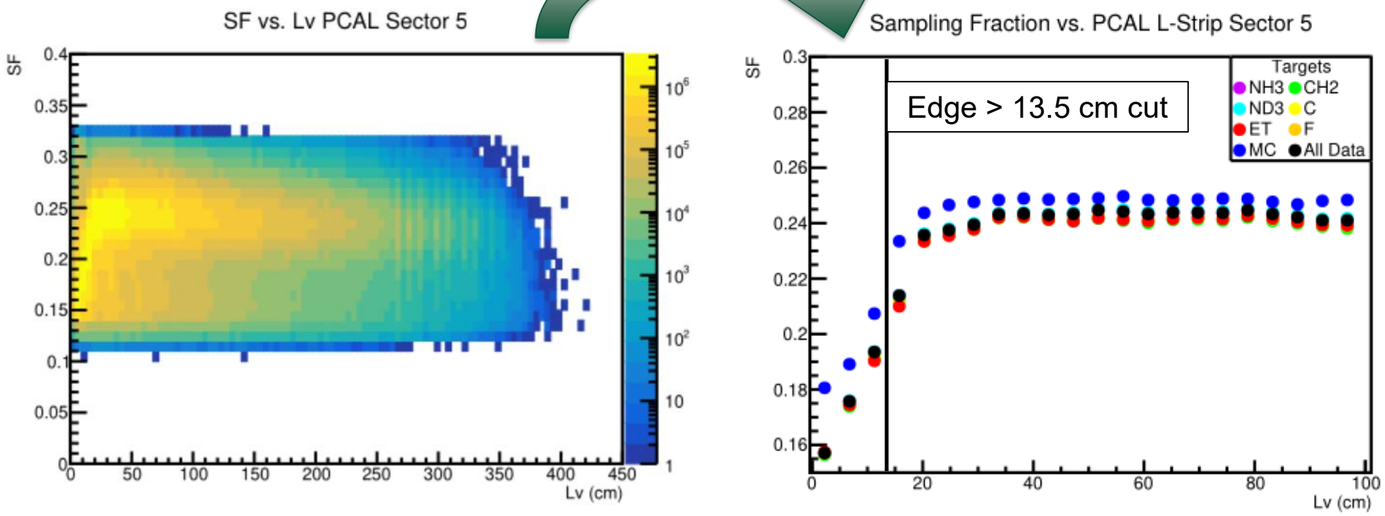

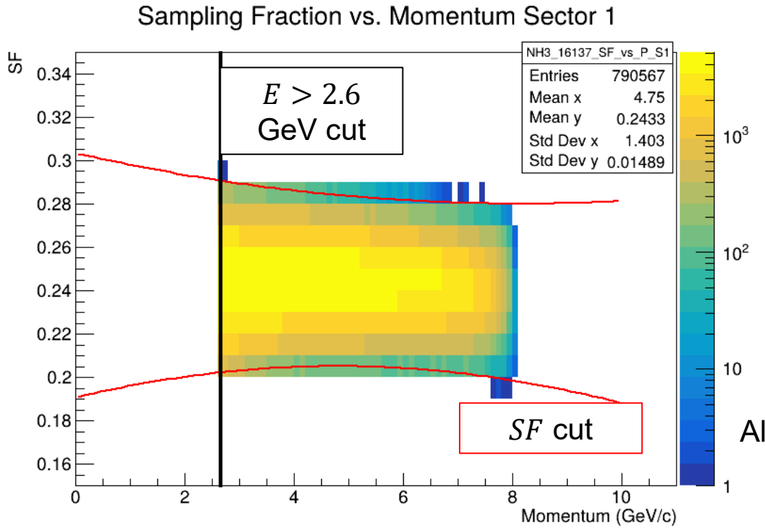

All kinematic and SF cuts applied to one sector

Calculating the Dilution Factor

- Each run period is divided into “epochs” based on when each target swap/anneal occurred
- Any movement of the target affects the packing fraction
- Using the measured counts, D_F were calculated for each epoch
- Mostly consistent across all epochs, except for positive solenoid data
- Some x-dependence in the P_F data

Summer 2022 Epochs

Epoch 1: 16137 – 16148
Epoch 2: 16156 – 16178
Epoch 3: 16213 – 16260
Epoch 4: 16318 – 16357
Epoch 5: 16658 – 16674
Epoch 6: 16675 – 16695
Epoch 7: 16709 – 16738
Epoch 8: 16742 – 16752
Epoch 9: 16753 – 16766
Epoch 10: 16767 – 16772

Fall 2022 (Neg. Sol.) Epochs

Epoch 11: 16983 – 16993
Epoch 12: 16995 - 17032
Epoch 13: 17067 – 17102
Epoch 14: 17144 – 17161
Epoch 15: 17162 – 17169

Fall 2022 (Pos. Sol.) Epochs

Epoch 16: 17188 – 17214
Epoch 17: 17215 – 17225
Epoch 18: 17353 – 17368
Epoch 19: 17371 – 17382

Spring 2023 Epochs

Epoch 20: 17575 – 17597
Epoch 21: 17598 – 17611
Epoch 22: 17720 – 17741
Epoch 23: 17748 – 17762

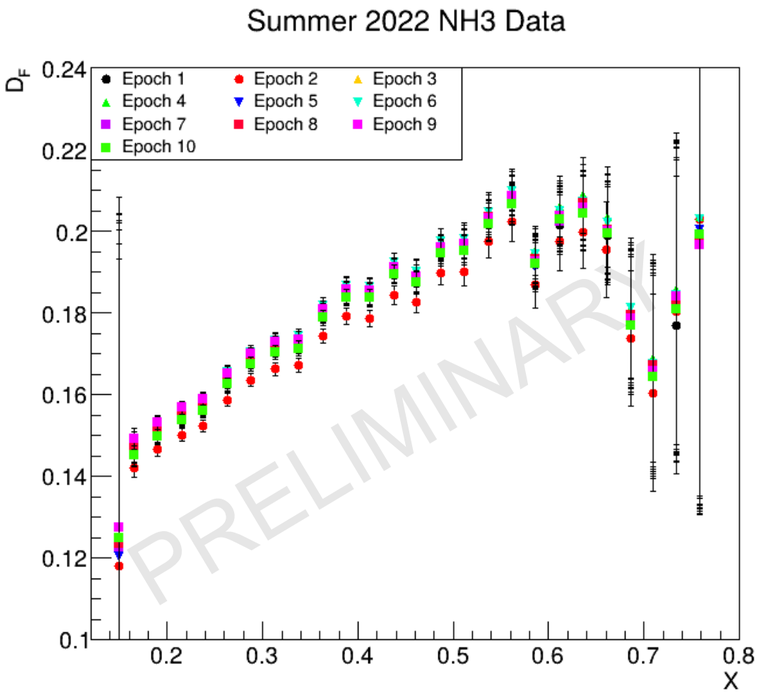

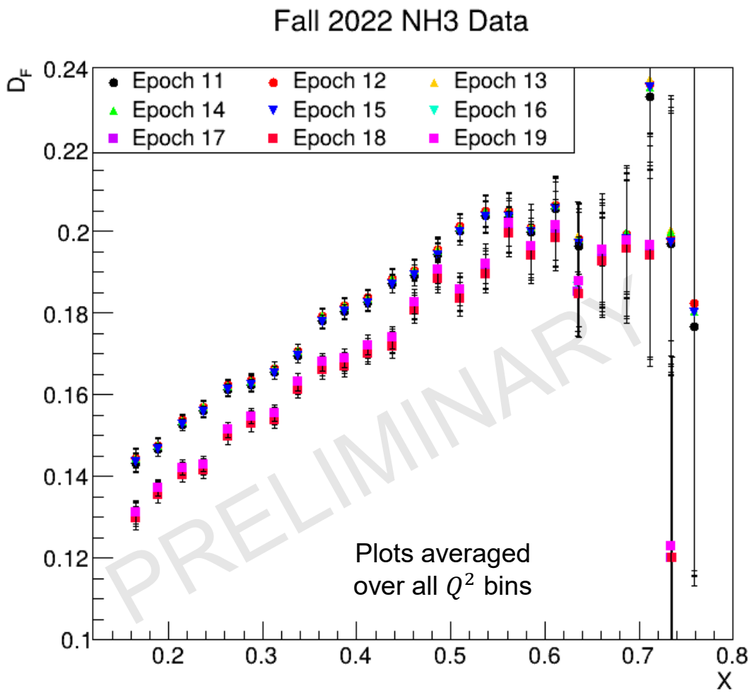

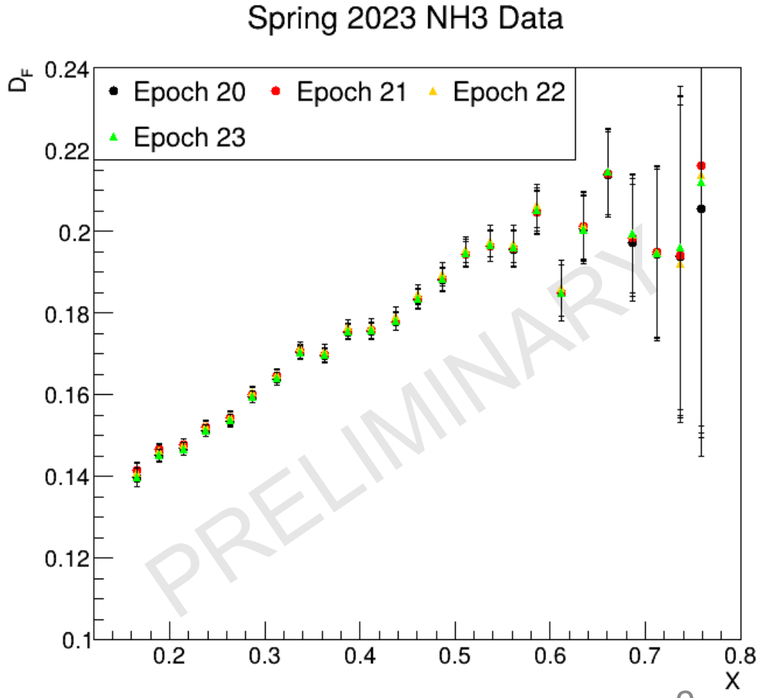

Calculating the Dilution Factor

- Each run period is divided into “epochs” based on when each target swap/anneal occurred
- Any movement of the target affects the packing fraction
- Using the measured counts, D_F were calculated for each epoch
- Mostly consistent across all epochs, except for positive solenoid data
- Some x-dependence in the P_F data

Summer 2022 Epochs

Epoch 1: 16137 – 16148
Epoch 2: 16156 – 16178
Epoch 3: 16213 – 16260
Epoch 4: 16318 – 16357
Epoch 5: 16658 – 16674
Epoch 6: 16675 – 16695
Epoch 7: 16709 – 16738
Epoch 8: 16742 – 16752
Epoch 9: 16753 – 16766
Epoch 10: 16767 – 16772

Fall 2022 (Neg. Sol.) Epochs

Epoch 11: 16983 – 16993
Epoch 12: 16995 - 17032
Epoch 13: 17067 – 17102
Epoch 14: 17144 – 17161
Epoch 15: 17162 – 17169

Fall 2022 (Pos. Sol.) Epochs

Epoch 16: 17188 – 17214
Epoch 17: 17215 – 17225
Epoch 18: 17353 – 17368
Epoch 19: 17371 – 17382

Spring 2023 Epochs

Epoch 20: 17575 – 17597
Epoch 21: 17598 – 17611
Epoch 22: 17720 – 17741
Epoch 23: 17748 – 17762

Summer 2022 NH3 Data

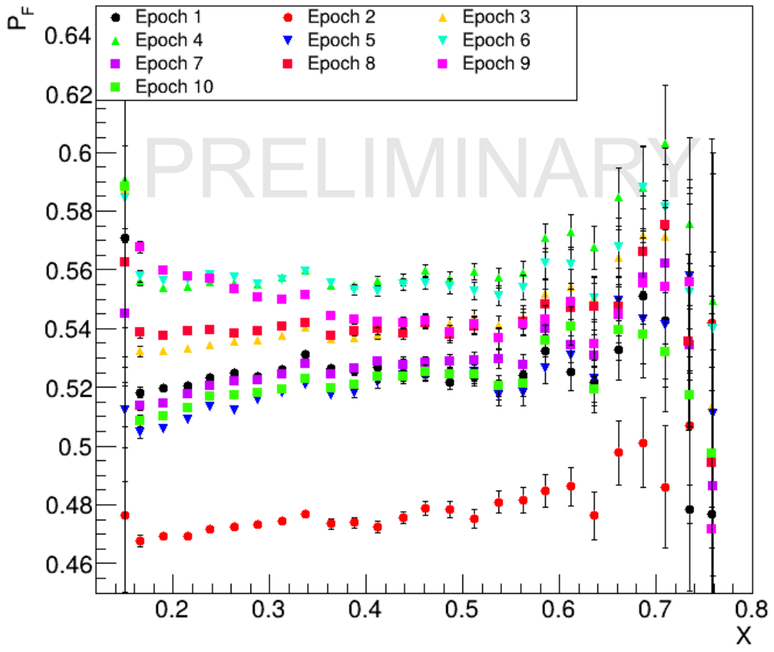

Fall 2022 NH3 Data

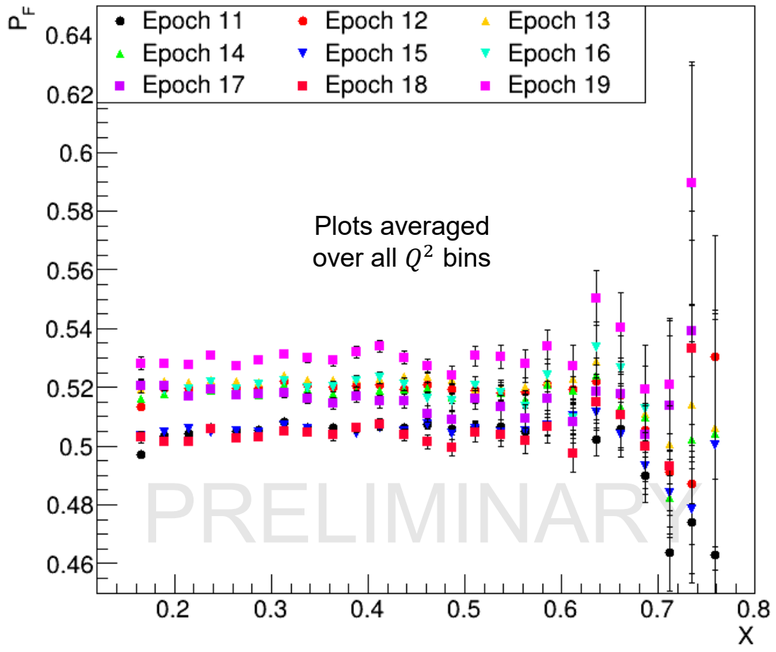

Spring 2023 NH3 Data

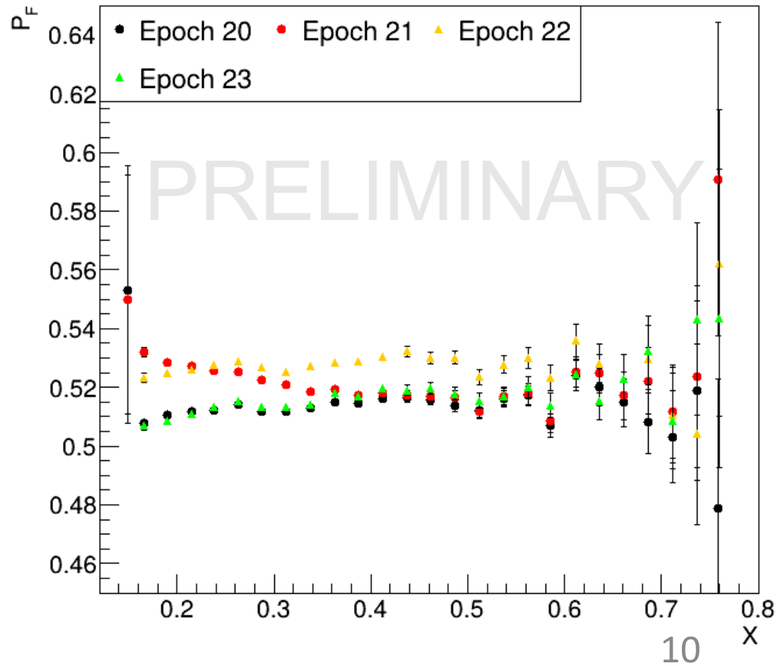

D_F Systematics: Thermal Contractions

- Target material geometries/densities were measured at roughly room temperature (300 K)
- However, cooling the targets to ~1 K in the liquid helium bath introduces thermal contractions, which affect the D_F and P_F
- Two primary unknowns for thermal contractions: expansion constant $\boldsymbol{\alpha}$ and target anisotropic behavior $\boldsymbol{\beta}$

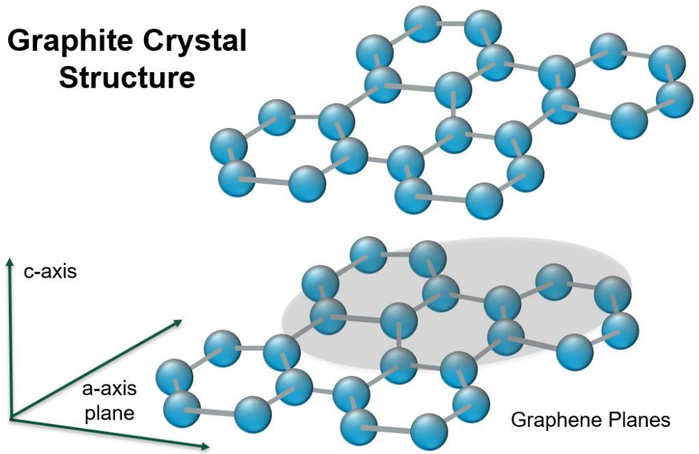

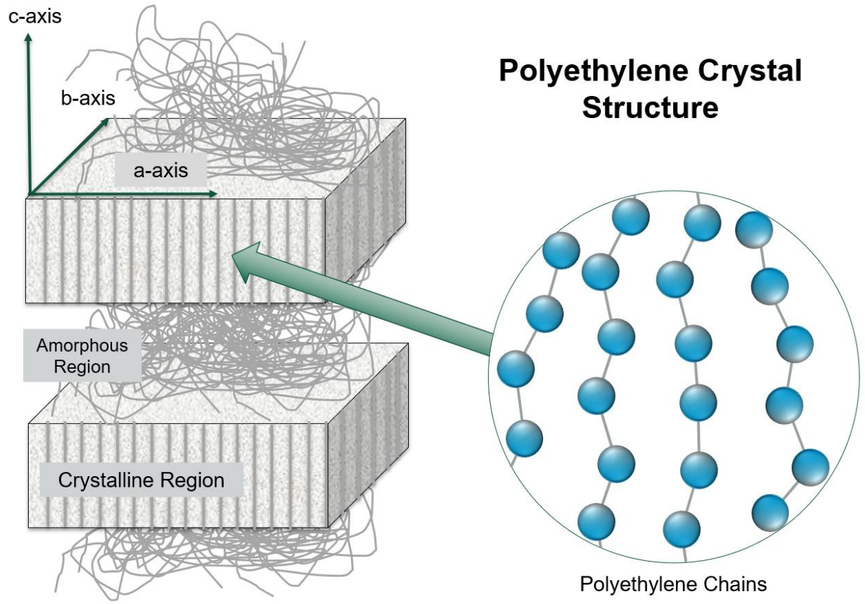

PE crystalline structure information from van Dorp et. al. [Ref. 5]

- Graphite (GR) and polyethylene (PE) targets have a crystalline structure
- Potential for anisotropic behavior during thermal contraction ⇒ different effects on areal density
- Accounted for unknown $\boldsymbol{\alpha}, \boldsymbol{\beta}$ in the systematic error

Radial Contraction (*R*)

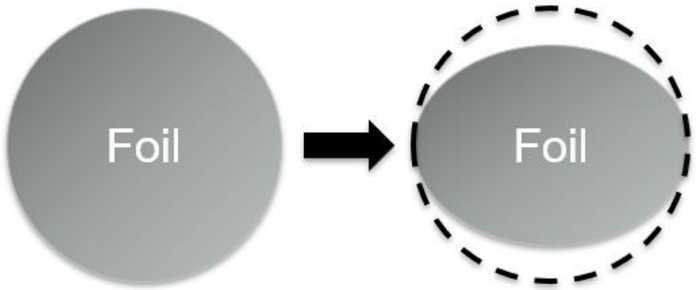

(GR)

Length Contraction (*L*)

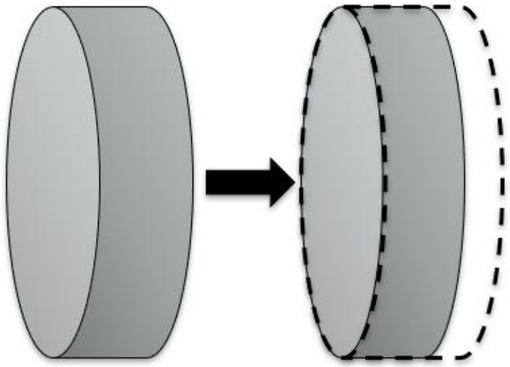

(GR)

Isotropic Contraction (*Iso*)

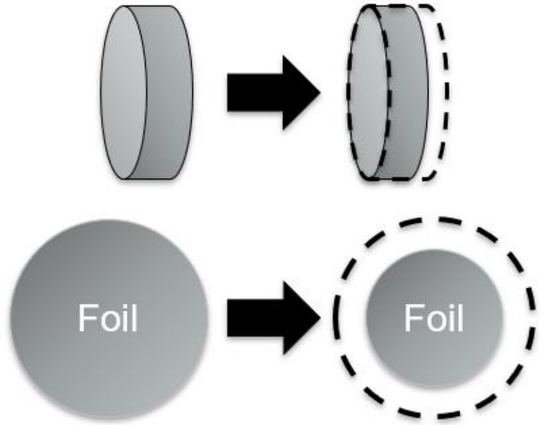

(GR)

Radius + Length Contraction (*RL*)

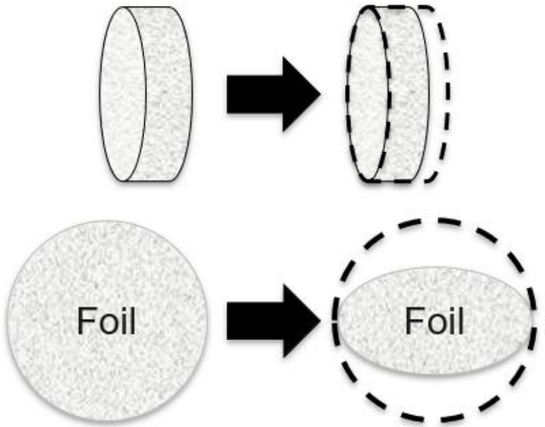

(PE)

Both Radii Contraction (*RR*)

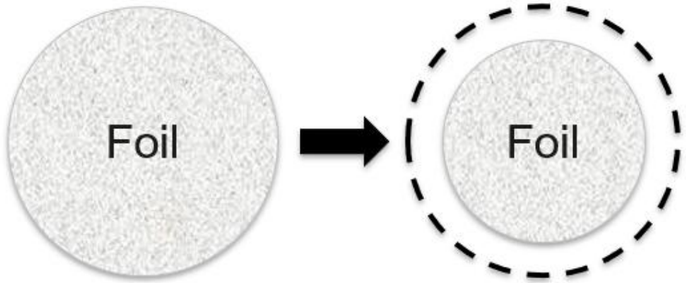

(PE)

Isotropic Contraction (*Iso*)

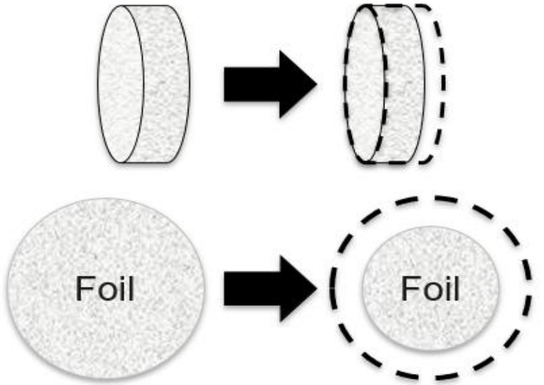

(PE)

- Graphite (GR) and polyethylene (PE) targets have a crystalline structure
- Potential for anisotropic behavior during thermal contraction ⇒ different effects on areal density
- Accounted for unknown $\boldsymbol{\alpha, \beta}$ in the systematic error

D_F Systematic Errors

- Systematic errors in D_F and P_F determined through an iterative process of varying material contractions by $\boldsymbol{\alpha}$ and $\boldsymbol{\beta}$
  1. Holding all other material properties at their measured room temperature values, the D_F and P_F were recalculated across all variations of a material's $\boldsymbol{\alpha}$ and $\boldsymbol{\beta}$
  2. For every bin in x, Q^2 the standard deviation across all variations was calculated
  3. The standard deviation was taken as the systematic error for that bin
  4. Systematic errors were parameterized using a quadratic (for D_F) equation or a constant (for P_F)

- Very large systematic errors in D_F for CH2, from **9% at small x to 6% at large x**

Thermal Contraction Parameters By Material				
Target Material	α-Range (%)	β Configurations	δ_{sys}-Range D_F (%)	δ_{sys}-Range P_F (%)
PE (CH_2)	1.5, 2.0, 2.5, 3.0	RR, RL, Iso	6%-9%	2.2%
Graphite	0.3, 0.5, 0.7, 0.9, 1.2, 1.5	R, L, Iso	2.5%-4%	0.2%
Teflon	1.7, 1.8, 1.9, 2.0, 2.1	Iso	<0.1%	0.16%
Ammonia	$\pm1, \pm2, \pm3, \pm4, \pm5$	Iso	0.5%	4%
PE (Low Estimate)	1.5, 2.0, 2.5	RR, RL, Iso	4.5%-7%	1.8%
Graphite (Low Estimate)	0.3, 0.5, 0.7, 0.9	R, L, Iso	2%-2.5%	0.14%

Graphite and PE expansion values α taken from [Ref. 6]
Teflon expansion values taken from [Ref. 7]

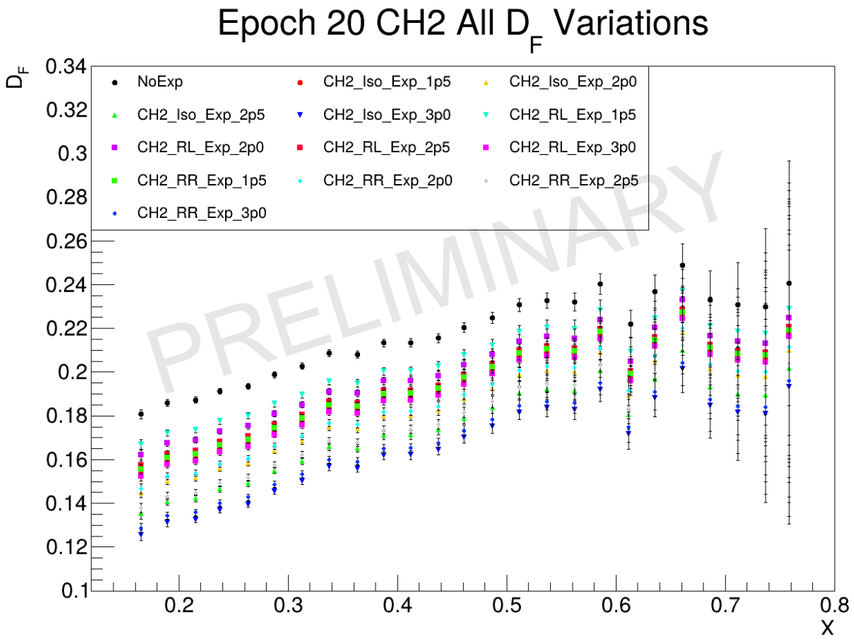

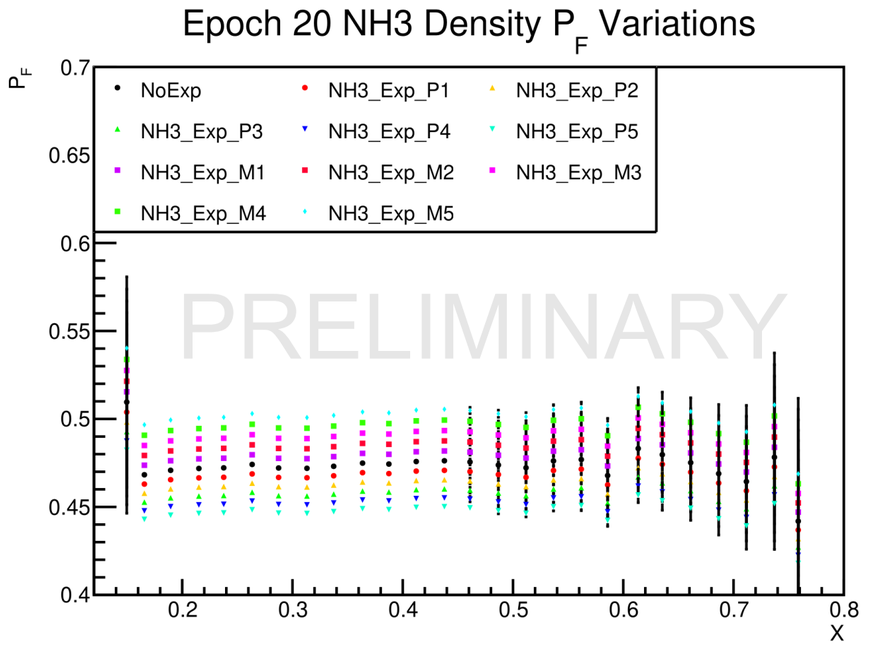

D_F Systematic Errors

- Systematic errors in D_F and P_F determined through an iterative process of varying material contractions by $\boldsymbol{\alpha}$ and $\boldsymbol{\beta}$
  1. Holding all other material properties at their measured room temperature values, the D_F and P_F were recalculated across all variations of a material's $\boldsymbol{\alpha}$ and $\boldsymbol{\beta}$
  2. For every bin in x, Q^2 the standard deviation across all variations was calculated
  3. The standard deviation was taken as the systematic error for that bin
  4. Systematic errors were parameterized using a quadratic (for D_F) equation or a constant (for P_F)

- Very large systematic errors in D_F for CH2, from **9% at small x to 6% at large x**

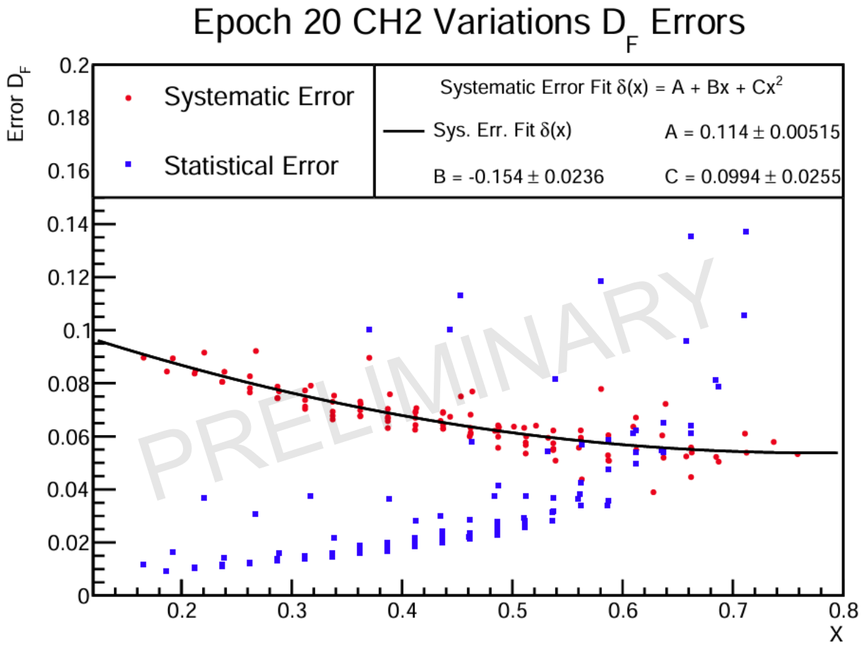

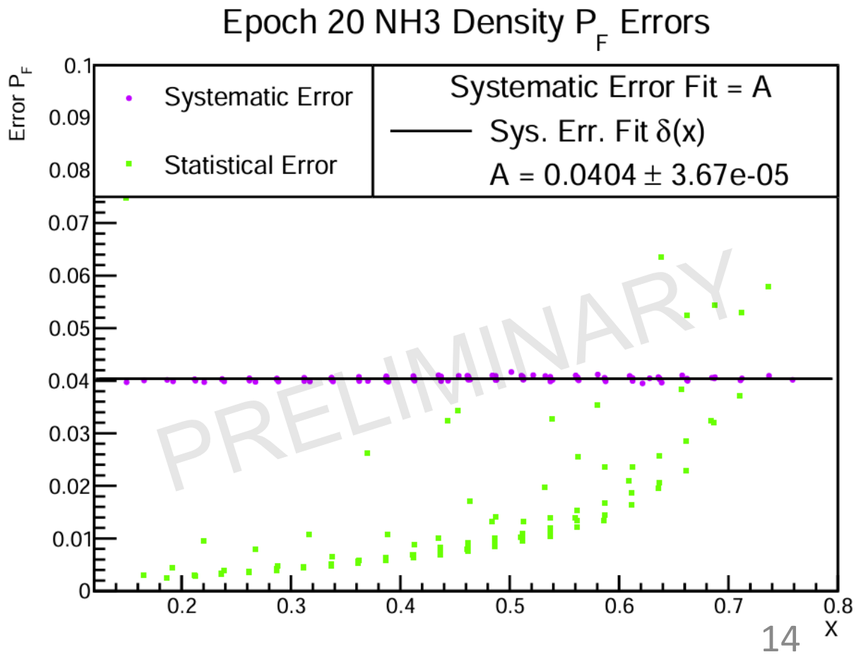

Thermal Contraction Parameters By Material				
Target Material	α-Range (%)	β Configurations	δ_{sys}-Range D_F (%)	δ_{sys}-Range P_F (%)
PE (CH_2)	1.5, 2.0, 2.5, 3.0	RR, RL, Iso	6%-9%	2.2%
Graphite	0.3, 0.5, 0.7, 0.9, 1.2, 1.5	R, L, Iso	2.5%-4%	0.2%
Teflon	1.7, 1.8, 1.9, 2.0, 2.1	Iso	<0.1%	0.16%
Ammonia	$\pm1, \pm2, \pm3, \pm4, \pm5$	Iso	0.5%	4%
PE (Low Estimate)	1.5, 2.0, 2.5	RR, RL, Iso	4.5%-7%	1.8%
Graphite (Low Estimate)	0.3, 0.5, 0.7, 0.9	R, L, Iso	2%-2.5%	0.14%

Graphite and PE expansion values α taken from [Ref. 6]
Teflon expansion values taken from [Ref. 7]

Measurement of Thermal α and β

- Prompted a direct measurement of CH2 and graphite samples
- Samples were made from the same extruded rods that the CH2 and graphite target foils were taken from
- Two 20mm x 20mm samples of each material
- Thermal contraction measured from room temperature (~300K) to liquid nitrogen (~77K)
  1. Measured diameter and length of each sample at room temperature
  2. Immerse in liquid nitrogen until cooled, and then measure again, holding it within the liquid nitrogen vapor
- Final values of $\boldsymbol{\alpha}$ for length and diameter taken as the average between each of the two samples

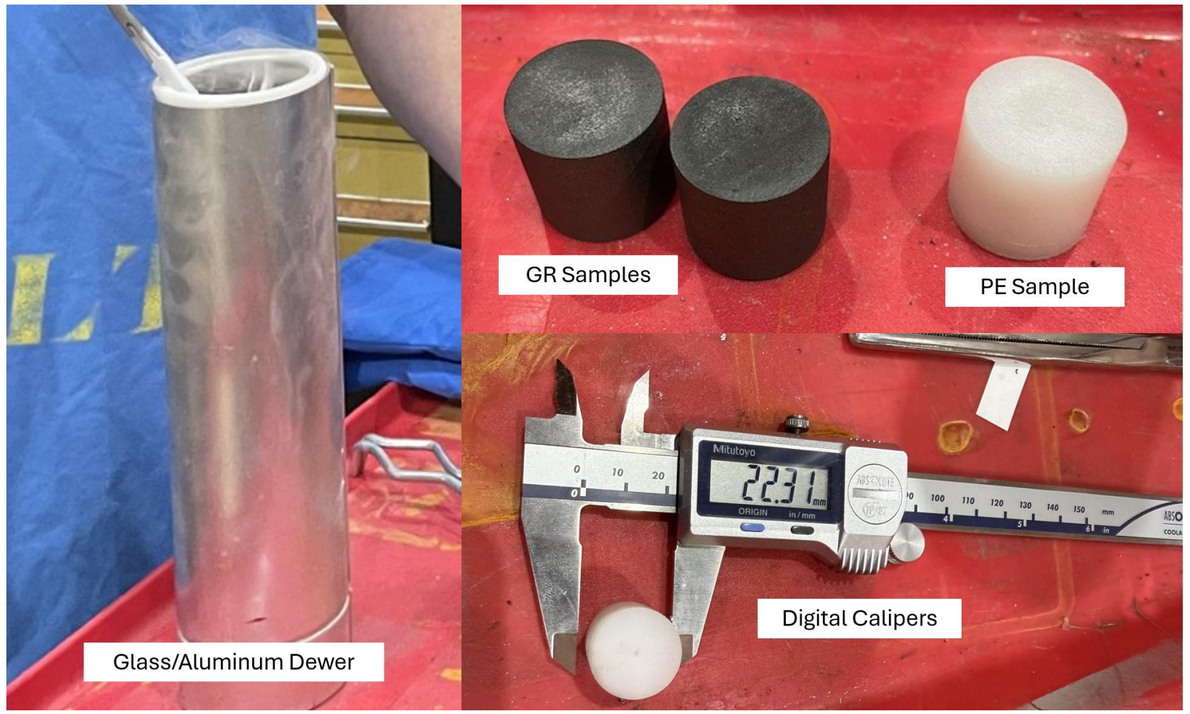

Measured Thermal Contractions			
Polyethylene (CH2)		**Graphite (Carbon)**	
α_D (Diameter)	**α_L (Length)**	**α_D (Diameter)**	**α_L (Length)**
1.75%	2.06%	-0.45%	-0.26%

Thanks to James Maxwell, Chris Keith, and James Brock for making the samples!!!
Thanks to Sailaja, Stephen, and James Maxwell for helping take the measurements!!!

Measurement of Thermal α and β

- CH2 measurement saw anisotropic behavior; graphite possibly expanded slightly as it cooled
- Results extrapolated to ~1K bath temperature through $\boldsymbol{\alpha} \rightarrow \alpha/0.9$, $\alpha/0.8$
- Assumes that roughly 80-90% of material thermal contraction (from room temperature) occurs by liquid nitrogen temperatures [Ref. 6]
- Repeated systematic error study using smaller ranges of $\boldsymbol{\alpha}$ constrained to one $\boldsymbol{\beta}$ configuration:
  - Lower estimate: $\alpha, \alpha/0.95, \alpha/0.9$
  - Larger estimate: $\alpha, \alpha/0.95, \alpha/0.9, \alpha/0.85, \alpha/0.8$
- CH2 systematics recalculated to be below 1-2% at large x
- Plans to repeat measurements more carefully on CH2 and graphite
  - Verify method by measuring thermal contraction of a known material (like aluminum)
  - Better understand anisotropy in graphite areal density
  - Get measurements of CD2 foil – because of different manufacturing than CH2, we expect different $\boldsymbol{\alpha}$

FIGURE AND TABLE NO. 400R. RECOMMENDED VALUES FOR THERMAL LINEAR EXPANSION OF POLYETHYLENE

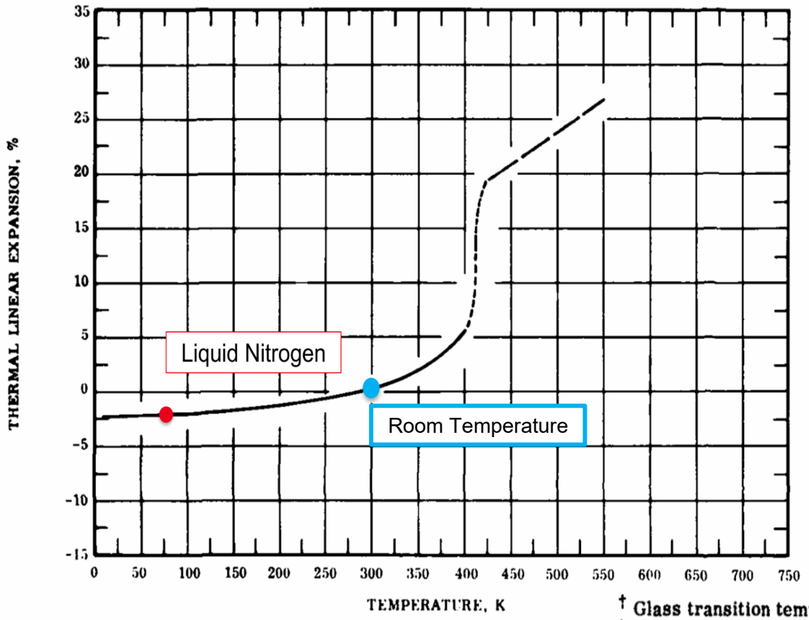

RECOMMENDED VALUES

[Temperature, T, K; Linear Expansion, $\Delta L/L_0$, %; α, 10^{-6} K^{-1}]

T	$\Delta L/L_0$	α
10	-2.44	12
25	-2.41	23
50	-2.34	33
75	-2.25	45
100	-2.12	56
150	-1.76	82
200	-1.30	110
250	-0.67	141
293	0.00	169
325	0.75	330
350	1.60	490
375	3.10	690
400†	5.60	940
425†	19.4‡	
450	21.0‡	
500	24.1‡	
550	27.5‡	

† Glass transition temperature.
‡ Provisional values.

N. B. of Standards, A compilation and evaluation of mechanical, thermal, and electrical properties of selected polymers (1973). {Ref. 6[

Measured Thermal Contractions			
Polyethylene (CH2)		Graphite (Carbon)	
α_D (Diameter)	α_L (Length)	α_D (Diameter)	α_L (Length)
1.75%	2.06%	-0.45%	-0.26%

Measurement of Thermal α and β

- CH2 measurement saw anisotropic behavior; graphite possibly expanded slightly as it cooled
- Results extrapolated to ~1K bath temperature through $\boldsymbol{\alpha} \rightarrow \alpha/0.9$, $\alpha/0.8$
- Assumes that roughly 80-90% of material thermal contraction (from room temperature) occurs by liquid nitrogen temperatures [Ref. 6]
- Repeated systematic error study using smaller ranges of $\boldsymbol{\alpha}$ constrained to one $\boldsymbol{\beta}$ configuration:
  - Lower estimate: α, $\alpha/0.95$, $\alpha/0.9$
  - Larger estimate: α, $\alpha/0.95$, $\alpha/0.9$, $\alpha/0.85$, $\alpha/0.8$
- CH2 systematics recalculated to be below 1-2% at large x
- Plans to repeat measurements more carefully on CH2 and graphite
  - Verify method by measuring thermal contraction of a known material (like aluminum)
  - Better understand anisotropy in graphite areal density
  - Get measurements of CD2 foil – because of different manufacturing than CH2, we expect different $\boldsymbol{\alpha}$

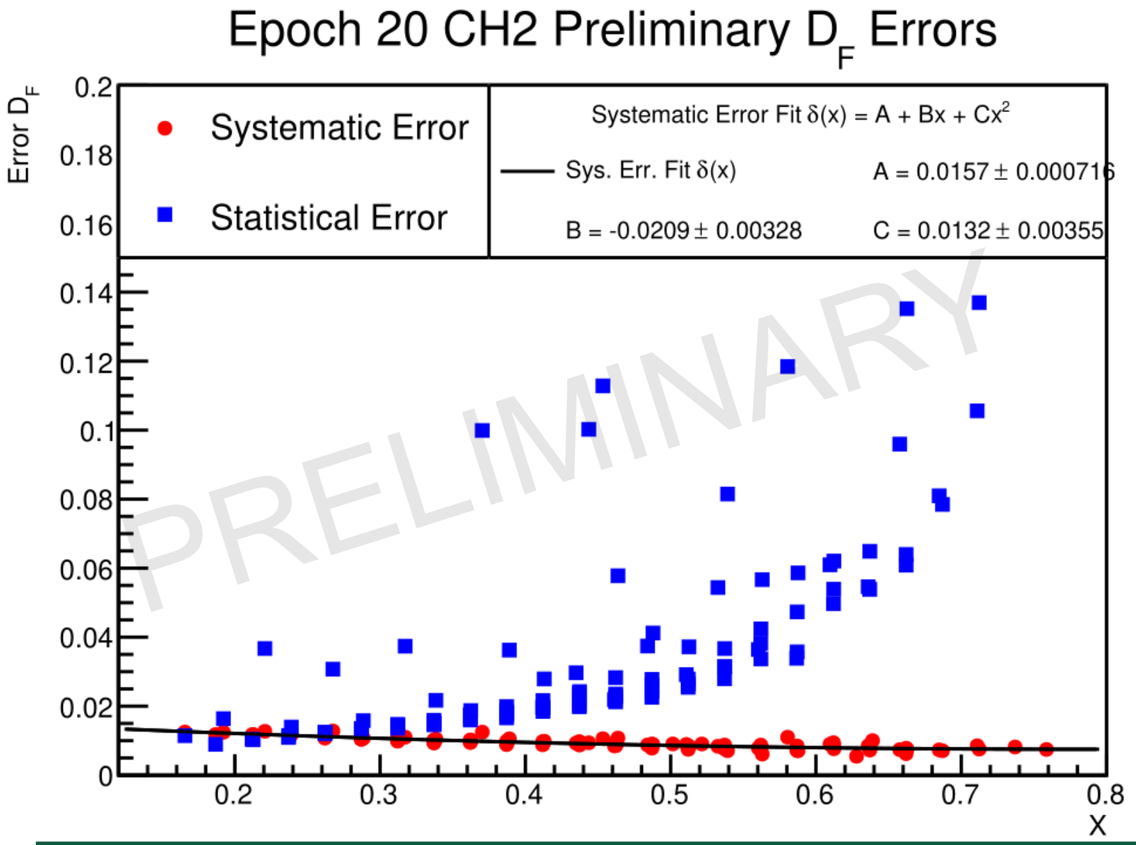

Measured Thermal Contractions			
Polyethylene (CH2)		Graphite (Carbon)	
α_D (Diameter)	α_L (Length)	α_D (Diameter)	α_L (Length)
1.75%	2.06%	-0.45%	-0.26%

Measurement of Thermal α and β

- CH2 measurement saw anisotropic behavior; graphite possibly expanded slightly as it cooled
- Results extrapolated to ~1K bath temperature through $\boldsymbol{\alpha} \rightarrow \alpha/0.9$, $\alpha/0.8$
- Assumes that roughly 80-90% of material thermal contraction (from room temperature) occurs by liquid nitrogen temperatures [Ref. 6]
- Repeated systematic error study using smaller ranges of $\boldsymbol{\alpha}$ constrained to one $\boldsymbol{\beta}$ configuration:
  - Lower estimate: α, $\alpha/0.95$, $\alpha/0.9$
  - Larger estimate: α, $\alpha/0.95$, $\alpha/0.9$, $\alpha/0.85$, $\alpha/0.8$
- CH2 systematics recalculated to be below 1-2% at large x
- Plans to repeat measurements more carefully on CH2 and graphite
  - Verify method by measuring thermal contraction of a known material (like aluminum)
  - Better understand anisotropy in graphite areal density
  - Get measurements of CD2 foil – because of different manufacturing than CH2, we expect different $\boldsymbol{\alpha}$

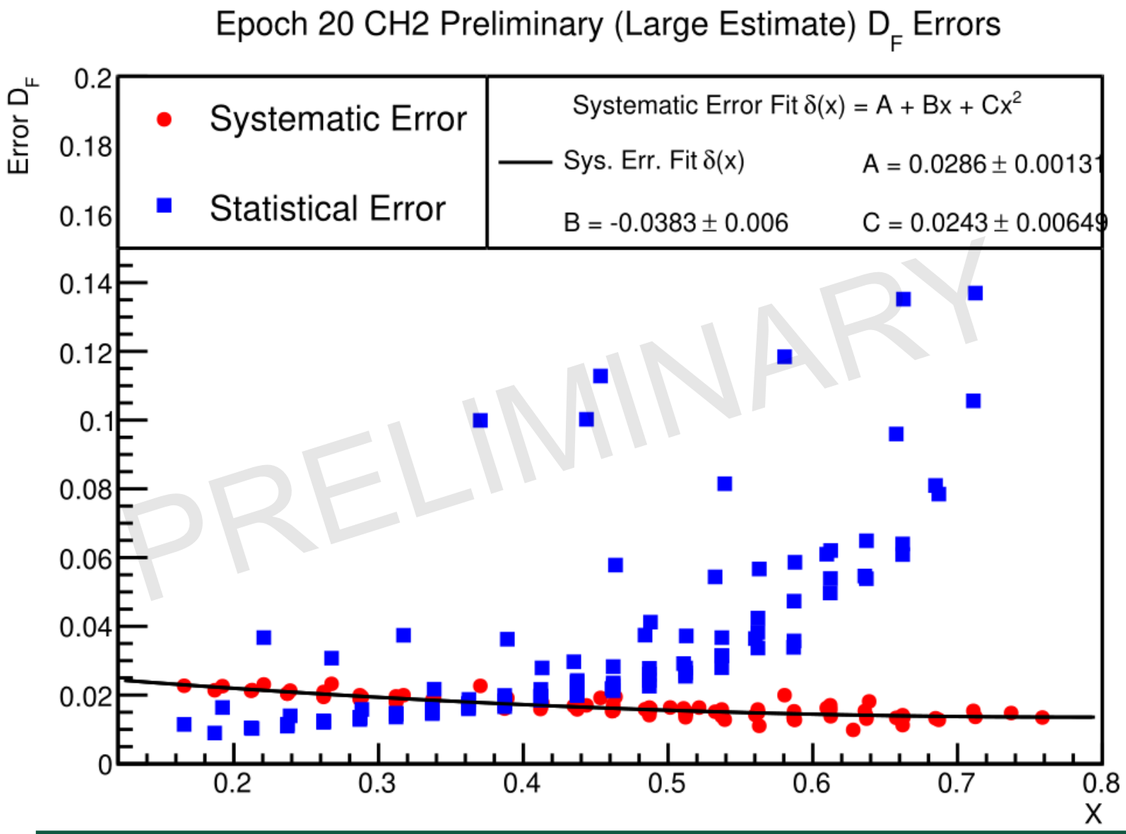

Measured Thermal Contractions			
Polyethylene (CH2)		**Graphite (Carbon)**	
α_D (Diameter)	**α_L (Length)**	**α_D (Diameter)**	**α_L (Length)**
1.75%	2.06%	-0.45%	-0.26%

Calculation of $P_b P_t$

- The beam and target polarization are calculated using the maximum likelihood method ⇒ what values of $P_b P_t$ are most likely to reproduce the data set?
- The maximum likelihood method is used to calculate $P_b P_t$ for each run:

$$(P_b P_t)_{DIS} = \frac{\sum_{x,Q^2} D_F A_{||,model}\left(N^{\downarrow\uparrow} - N^{\uparrow\uparrow}\right)}{\sum_{x,Q^2}\left(D_F A_{||,model}\right)^2 \left(N^{\downarrow\uparrow} + N^{\uparrow\uparrow}\right)}$$

$$\sigma_{PbPt} = \sqrt{\left(\sum_{x,Q^2}\left(N^{\downarrow\uparrow} + N^{\uparrow\uparrow}\right)\left(D_F A_{||,model}\right)^2\right)^{-1}}$$

- Where all data comes from the DIS channel, and N are the raw counts NOT normalized to the FC charge (due to FC charge asymmetry issues)
- $A_{||,model}$ is based on a fit to the world data of A_1, A_2, and R
- $A_{||,model} = D(A_1 + \eta A_2)$
- This introduces a model dependence on the calculation

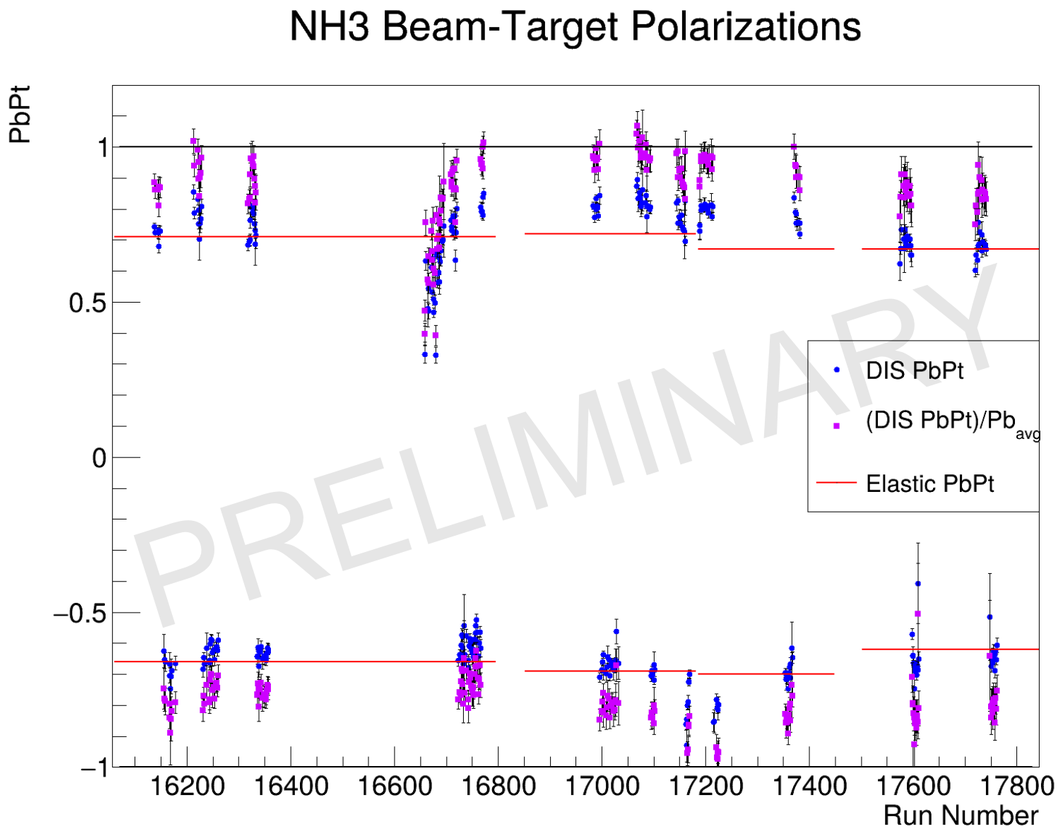

Calculation of $P_b P_t$

- To avoid model influence on $P_b P_t$, calculate a ***P***olarization ***N***ormalization ***F***actor (***PNF***) defined relative to elastic asymmetry $A_{||,el}$

$$\boldsymbol{PNF} = \frac{\sum_{Q^2} A_{||,el} \sum_{i=0}^{n_{runs}} \left(N_{el,i}^{\downarrow\uparrow} - N_{el,i}^{\uparrow\uparrow}\right) f_i (P_b P_t)_{DIS,i}}{\sum_{Q^2} \left(A_{||,el}\right)^2 \sum_{i=0}^{n_{runs}} \left(N_{el,i}^{\downarrow\uparrow} + N_{el,i}^{\uparrow\uparrow}\right) \left(f_i (P_b P_t)_{DIS,i}\right)^2}$$

$$\sigma_{PNF} = \sqrt{\left(\sum_{Q^2} \left(A_{||,el}\right)^2 \sum_{i=0}^{n_{runs}} \left(N_{el,i}^{\downarrow\uparrow} + N_{el,i}^{\uparrow\uparrow}\right) \left(f_i (P_b P_t)_{DIS,i}\right)^2 \right)^{-1}}$$

- Where $N_{el,i}$ are the counts from elastic ep scattering, f_i are the elastic dilution factors
- This is still a work in progress, so the results I'll show today use the unnormalized $(P_b P_t)_{DIS}$

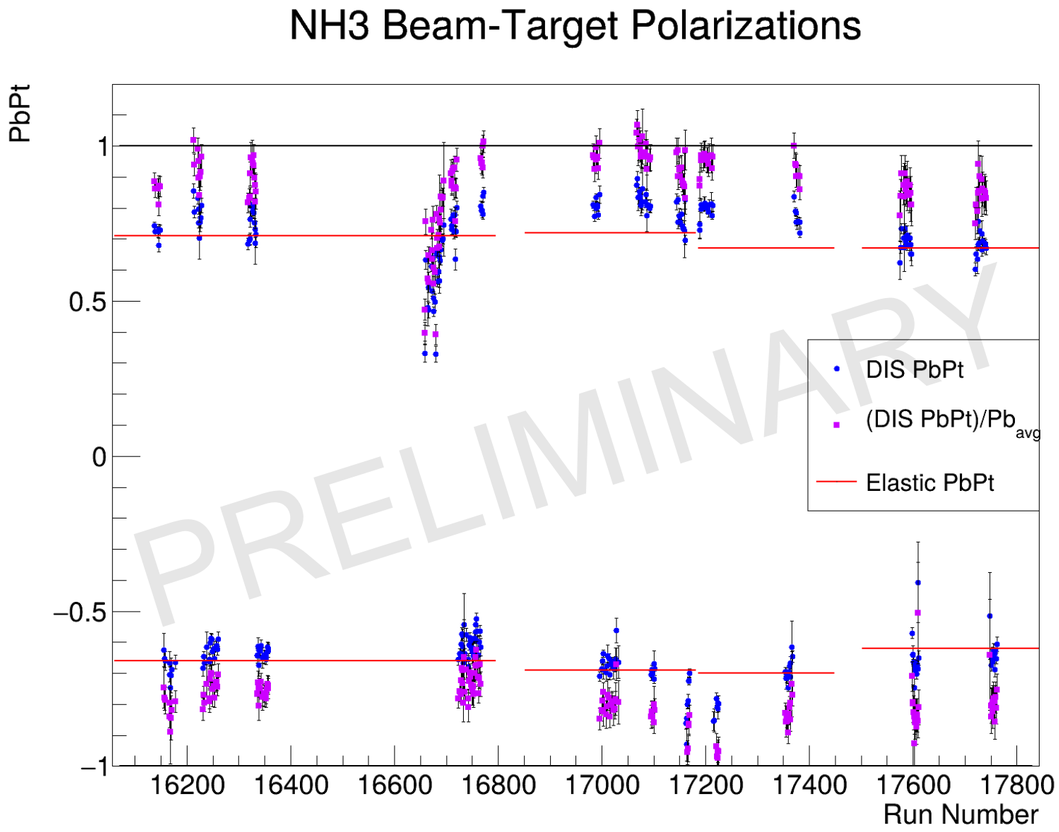

Preliminary Results for $A_{1,p}$

- The maximum likelihood method can also be used to combine the physical asymmetries $A_{||,meas}$ across all individual runs

$$A_{||,meas}(x,Q^2) = \frac{\sum_{i=0}^{n_{runs}} \left(N_i^{\downarrow\uparrow}(x,Q^2) - N_i^{\uparrow\uparrow}(x,Q^2)\right) D_{F,i}(x,Q^2)\boldsymbol{P_i}}{\sum_{i=0}^{n_{runs}} \left(N_i^{\downarrow\uparrow}(x,Q^2) + N_i^{\uparrow\uparrow}(x,Q^2)\right) \left(D_{F,i}(x,Q^2)\boldsymbol{P_i}\right)^2}$$

$$\sigma_{Ameas} = \sqrt{\left(\sum_{x,Q^2}(N^{\downarrow\uparrow} + N^{\uparrow\uparrow})(D_F\boldsymbol{P_i})^2\right)^{-1}}$$

- Once data is combined, $A_{1,p}$ is extracted using model values of A_2 and R

$$A_{1,p}(x,Q^2) = A_{||,phys}(x,Q^2)/D \; -\eta A_2(x,Q^2)$$

- Very preliminary results for $A_{1,p}$, showing statistical error bars and expected systematic errors

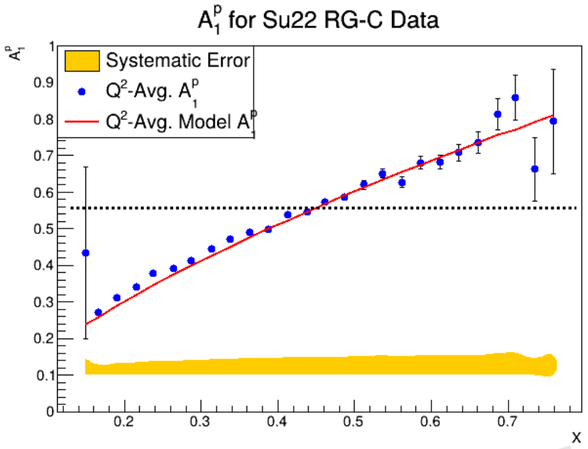

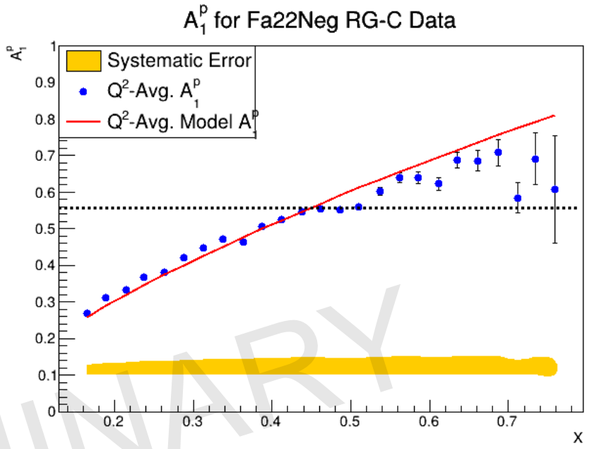

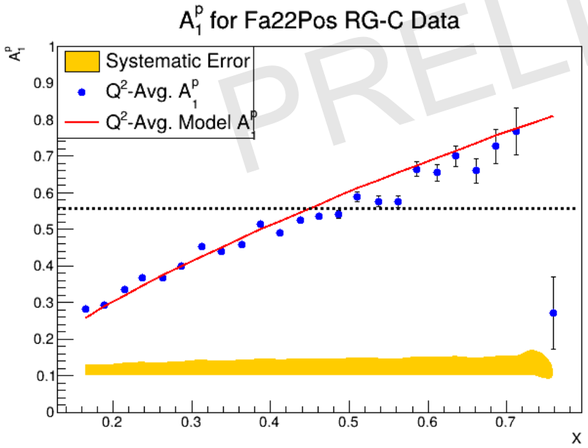

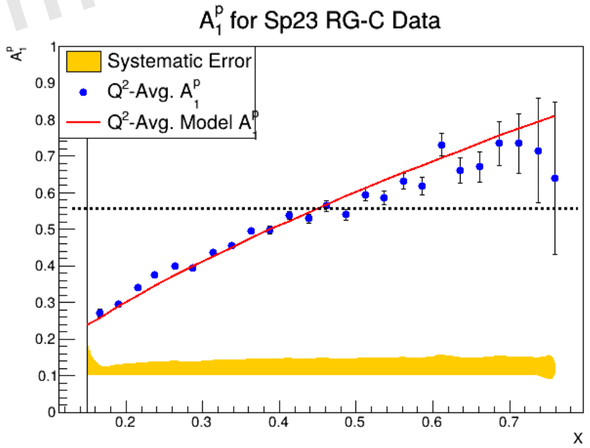

Preliminary Results for $A_{1,p}$

- The maximum likelihood method can also be used to combine the physical asymmetries $A_{||,meas}$ across all individual runs

$$A_{||,meas}(x,Q^2) = \frac{\sum_{i=0}^{n_{runs}} \left(N_i^{\downarrow\uparrow}(x,Q^2) - N_i^{\uparrow\uparrow}(x,Q^2)\right) D_{F,i}(x,Q^2)\boldsymbol{P_i}}{\sum_{i=0}^{n_{runs}} \left(N_i^{\downarrow\uparrow}(x,Q^2) + N_i^{\uparrow\uparrow}(x,Q^2)\right) \left(D_{F,i}(x,Q^2)\boldsymbol{P_i}\right)^2}$$

$$\sigma_{Ameas} = \sqrt{\left(\sum_{x,Q^2}(N^{\downarrow\uparrow} + N^{\uparrow\uparrow})(D_F\boldsymbol{P_i})^2\right)^{-1}}$$

- Once data is combined, $A_{1,p}$ is extracted using model values of A_2 and R

$$A_{1,p}(x,Q^2) = A_{||,phys}(x,Q^2)/D - \eta A_2(x,Q^2)$$

- Very preliminary results for $A_{1,p}$, showing statistical error bars and expected systematic errors

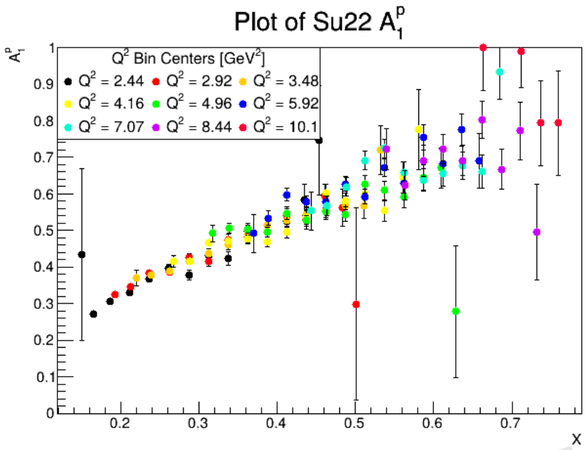

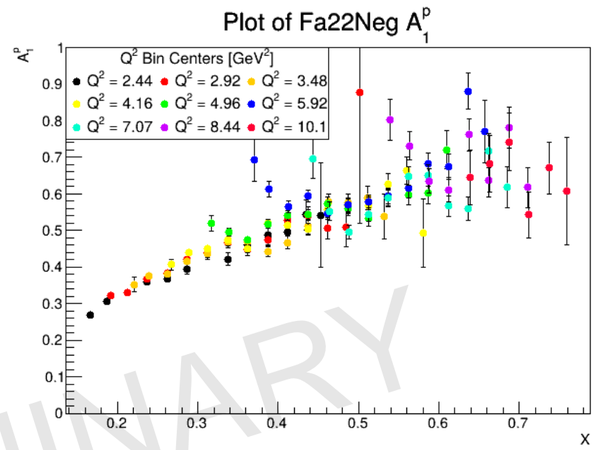

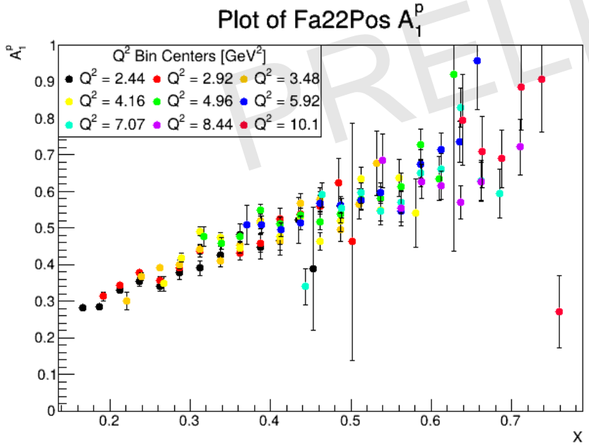

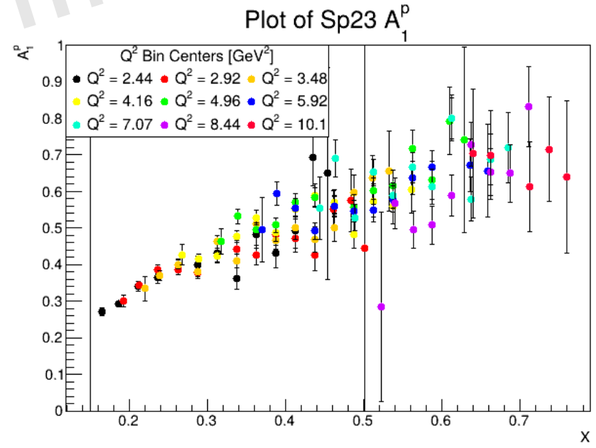

Preliminary Results for $A_{1,p}$

- The (non-exhaustive) list of work still to be done:
  1. Finalize the PNF calculation with elastics
  2. Finalize background contributions from polarization of ^{14}N and e^+e^- pair production
  3. Perform t-tests comparing run periods
  4. Corrections for FC charge asymmetries
  5. Radiative effects/corrections (for D_F and final results)
  6. Account for all systematic errors (thermal contractions, FC charge asymmetry)
- We hope to have more results by the fall collaboration meeting!

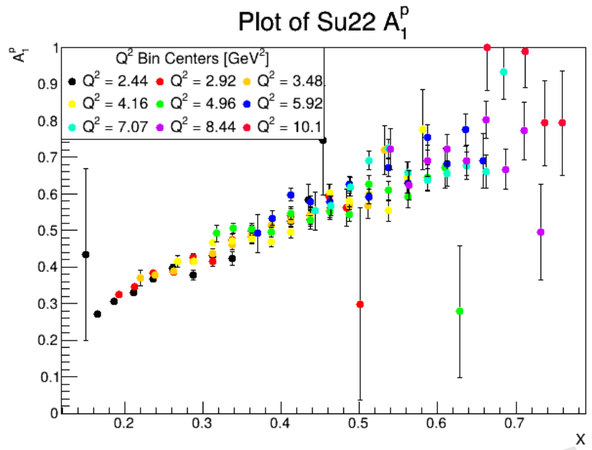

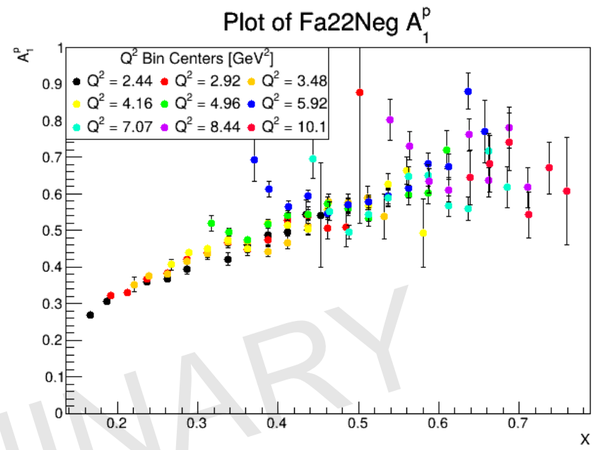

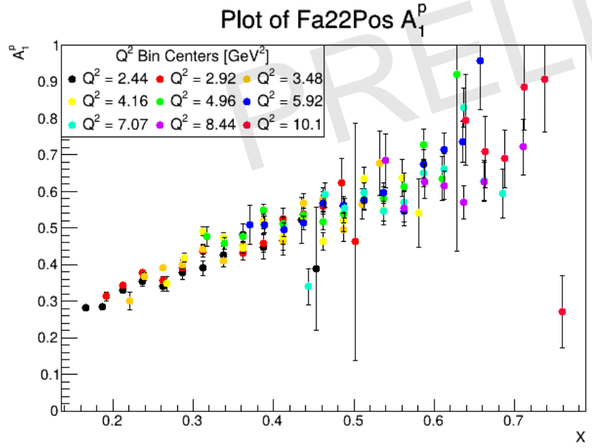

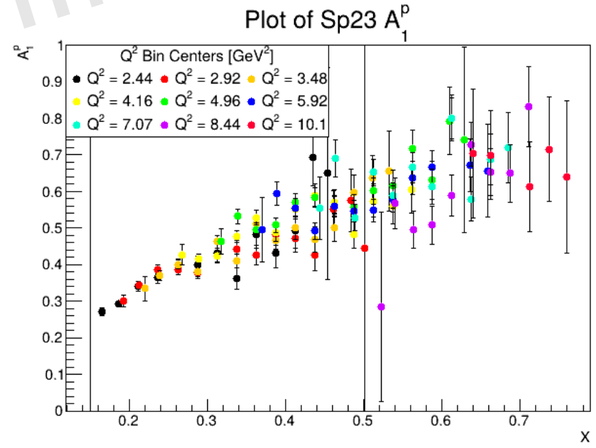

Any Questions?

References

1. M. Amarian et. al., “The Longitudinal Spin Structure of the Nucleon: A 12 GeV Research Proposal to Jefferson Lab (PAC 30)”. Link

2. V. Ziegler et. al. “The CLAS12 software framework and event reconstruction, Nuclear Instruments and Methods in Physics Research Section A: Accelerators, Spectrometers, Detectors and Associated Equipment”, 2020. Link

3. C. Keith et. al. “First use of a longitudinally polarized target with CLAS12”. Proceedings of 19th Workshop on Polarized Sources, Targets and Polarimetry - PoS(PSTP2022), 433, 009 (1-8). Link

4. J. Maxwell, “Polarized Targets at Jefferson Lab: Probing Nuclear Spin Structure”, New England Section, APS Meeting October 14th, 2022. Link

5. E. R. van Dorp et al., “Thermal expansion of semi-crystalline polymers: Anisotropic thermal strain and crystallite orientation”, Polymer, Volume 191, 2020, 122249, ISSN 0032-3861. Link

6. N. B. of Standards, A compilation and evaluation of mechanical, thermal, and electrical properties of selected polymers (1973). Link

7. Y. S. Touloukian et al., Thermophysical properties of matter - the tprc data series vol. 13. (1977). Link

8. N. Pilleux, “Nucleon structure studies at Jefferson Lab and the Electron-Ion Collider”, Universite Paris-Saclay, 2024. Link

Calculation of $A_{1,p}$

- The maximum likelihood method can also be used to combine the physical asymmetries $A_{||,meas}$ across all individual runs

$$A_{||,meas}(x,Q^2) = \frac{\sum_{i=0}^{nruns}\left(N_i^{\downarrow\uparrow}(x,Q^2) - N_i^{\uparrow\uparrow}(x,Q^2)\right)D_{F,i}(x,Q^2)\boldsymbol{P_i}}{\sum_{i=0}^{nruns}\left(N_i^{\downarrow\uparrow}(x,Q^2) + N_i^{\uparrow\uparrow}(x,Q^2)\right)\left(D_{F,i}(x,Q^2)\boldsymbol{P_i}\right)^2}, \quad \sigma_{Ameas} = \sqrt{\left(\sum_{x,Q^2}(N^{\downarrow\uparrow} + N^{\uparrow\uparrow})(D_F\boldsymbol{P_i})^2\right)^{-1}}$$

- Once data is combined, $A_{1,p}$ is extracted using model values of A_2 and R

$$A_{1,p}(x,Q^2) = A_{||,phys}(x,Q^2)/D \; -\eta A_2(x,Q^2)$$

- Modeling A_2, R introduces a small systematic effect

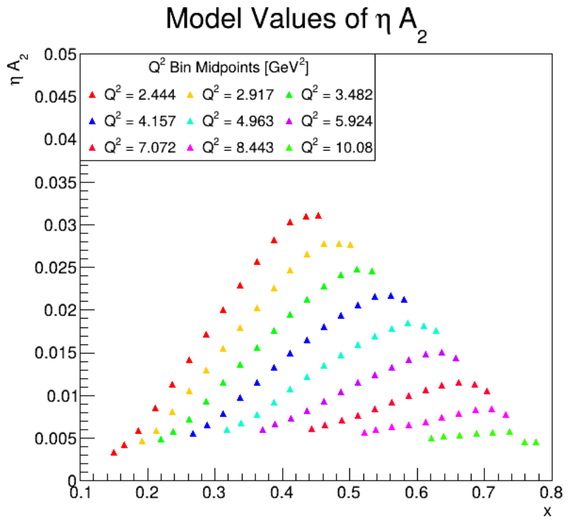

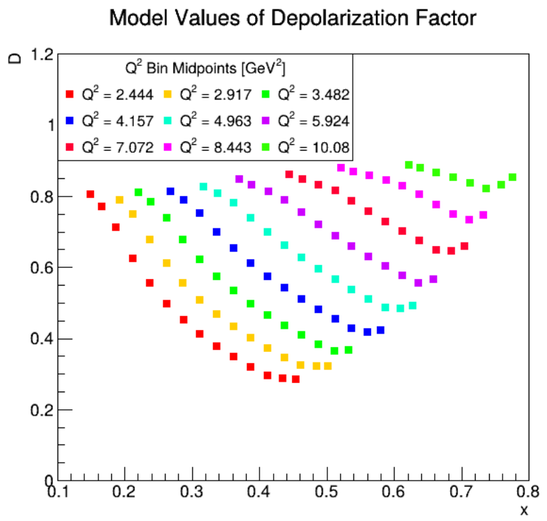

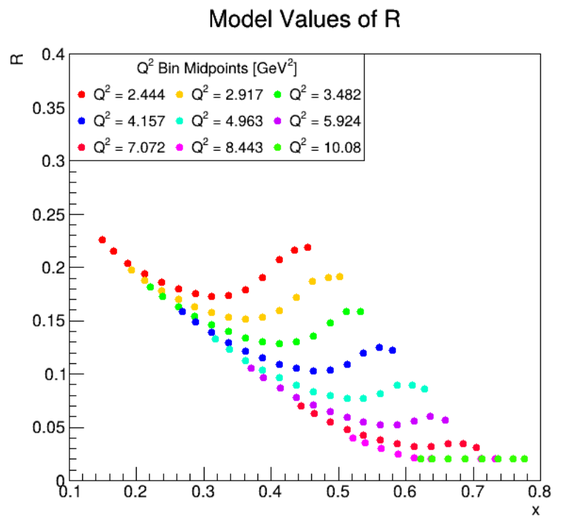

Note: The model values shown here are evaluated at the mean values of each x, Q^2 bin, ***NOT*** the bin midpoints listed in the legends.

Elastic ep Scattering

- Calculation of elastic quantities follows Noemie Pilleux's analysis
- Elastic double-spin asymmetry:

$$A_{||,el}(Q^2) = \frac{2\tau \frac{G_M}{G_E}\left(\frac{M}{E} + \frac{G_M}{G_E}\left[\frac{\tau M}{E} + (1+\tau)\tan^2(\theta/2)\right]\right)}{1 + \left(\frac{G_M}{G_E}\right)^2 \tau/\epsilon}$$

- ϵ = virtual photon polarization $= (1 + 2[1+\tau]\tan^2(\theta/2))^{-1}$, $\tau = Q^2/4M^2$, E = beam energy
- $G_{E,M}$ = Sachs form factors parameterized with Arrington model [ref]

- Elastic dilution factors determined via carbon subtraction
- $f = 1 - c\frac{N_C(Q^2)}{N_A(Q^2)}$, where N_C/N_A is the ratio of carbon to ammonia counts, $c = \frac{7}{6}\frac{\ell_A \rho_A}{\ell_C \rho_C}\frac{FC_A}{FC_C}$, $\ell_A = P_F * 2\text{cm}$

- Applied Pilleux's exclusivity cuts for the NH3 ep events:
  - 9.5 < E^{calc}_{beam} < 11.3 GeV ⇒ Reconstructed beam energy
  - $|MM^2_{ep\to ep}| < 0.05$ GeV^2 ⇒ Missing mass for ep scattering
  - $178° < \Delta\phi < 181°$ ⇒ Spread of expected ϕ (assuming elastic collision)
  - $|\delta P_p| < 0.5$ GeV/c ⇒ Difference between expected and measured proton momentum
  - $|\delta P_{e^-}| < 0.5$ GeV/c ⇒ Difference between expected and measured electron momentum

- Calculate normalized $P_b P_t$ for each run using $\boldsymbol{P} = (P_b P_t)_{DIS} * PNF$

Determining Cuts For DC

- The DC fiducial cuts based on average χ^2_{track}/NDF vs. edge variable of track position
- Cuts selected qualitatively based on where average χ^2 rises relative to the rest of the distribution
- Analyzed separately for inbending and outbending data using π^+, π^-
- Tracks binned in polar scattering angle θ, momentum P

- Iterative procedure for making cuts:
  1. First, make cuts for Region 3 using inbending data and cuts for Region 1 using outbending data
  2. After Region 1 and 3 cuts are applied, look at Region 2 and make cuts for inbending and outbending

- Also applied vertex cuts on X, Y, and Z
- Based on vertex distributions and target foil locations

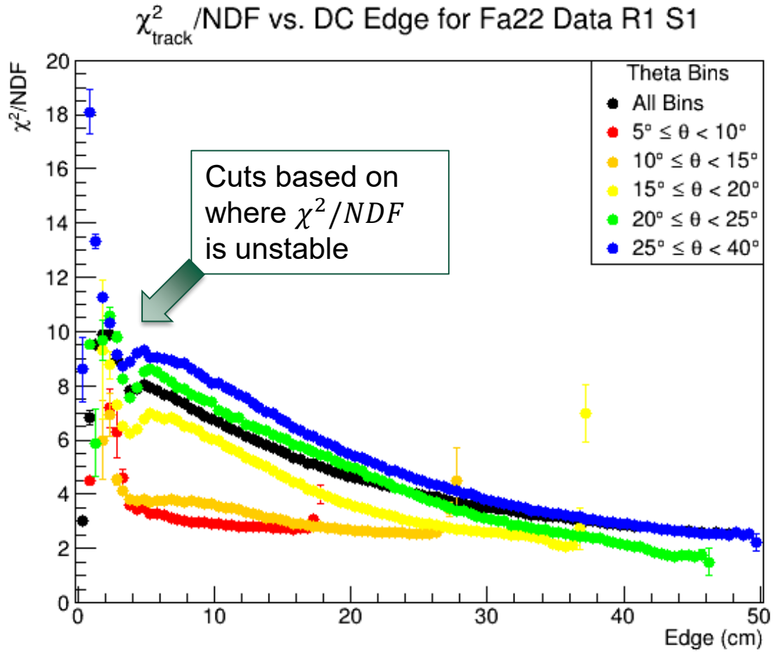

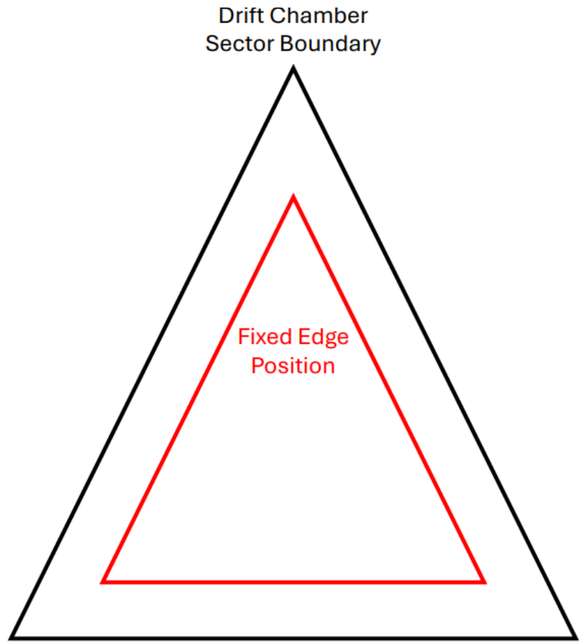

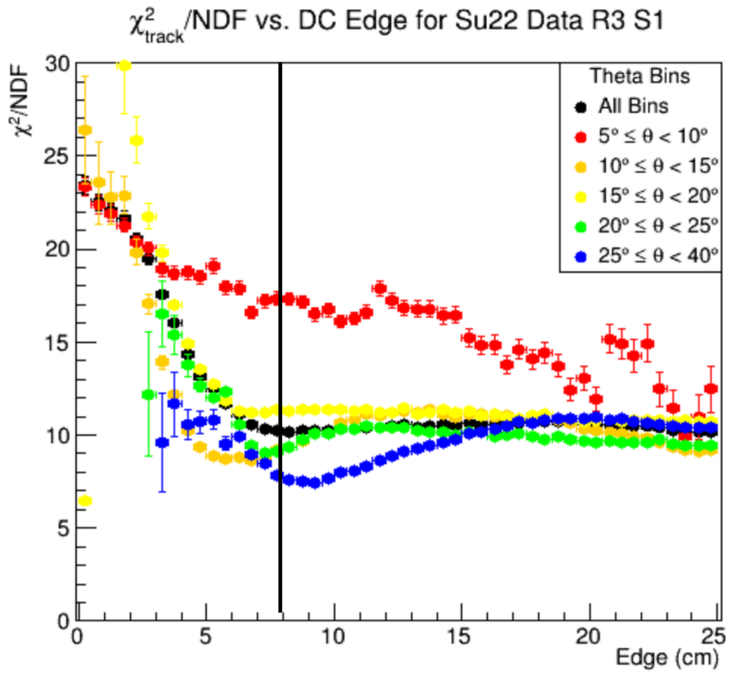

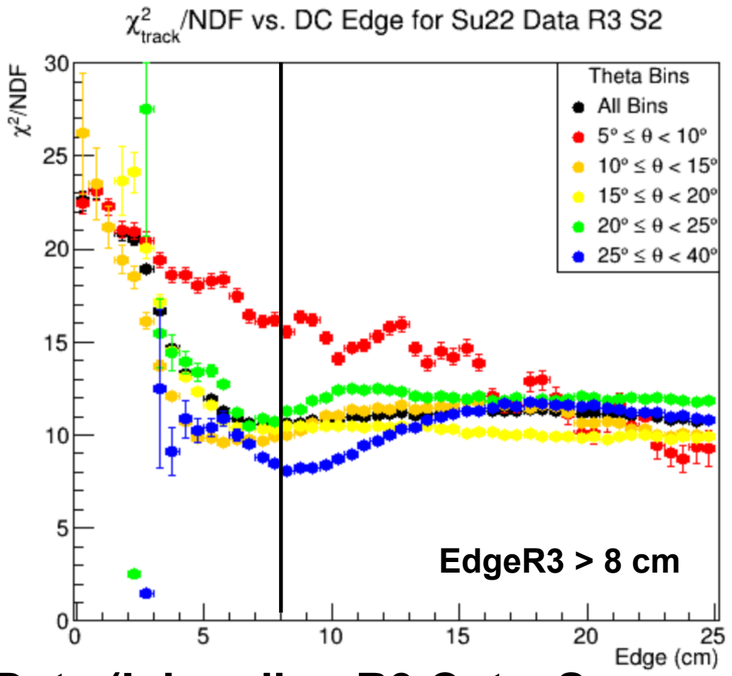

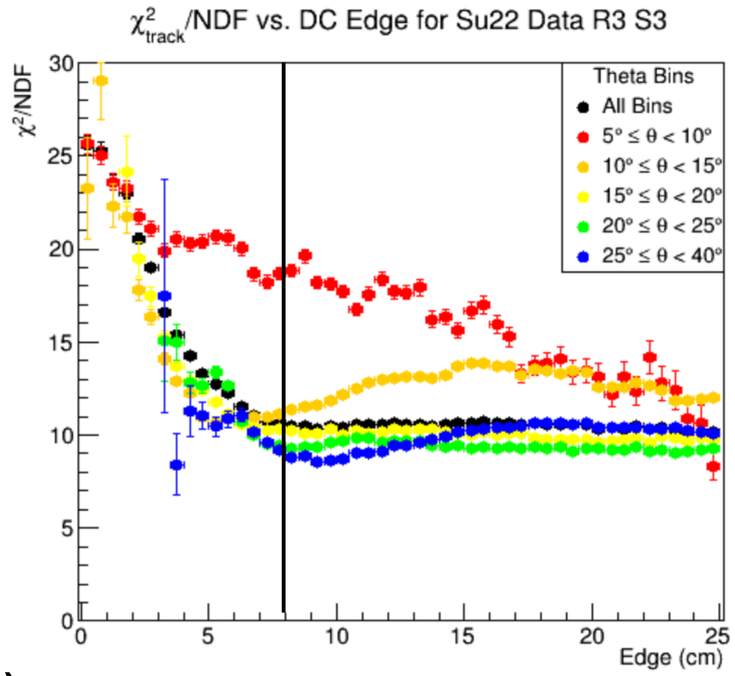

π^- Data (Inbending R3 Cuts, Summer 2022)

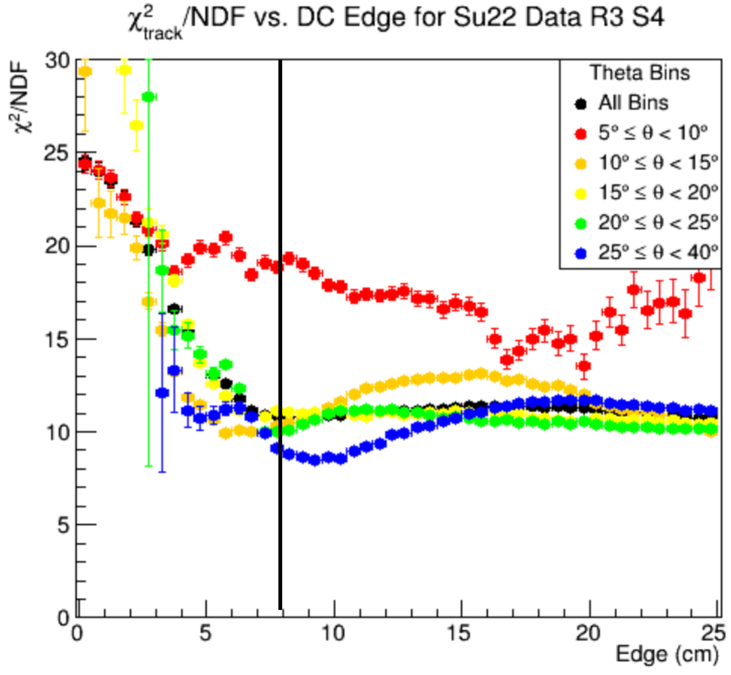

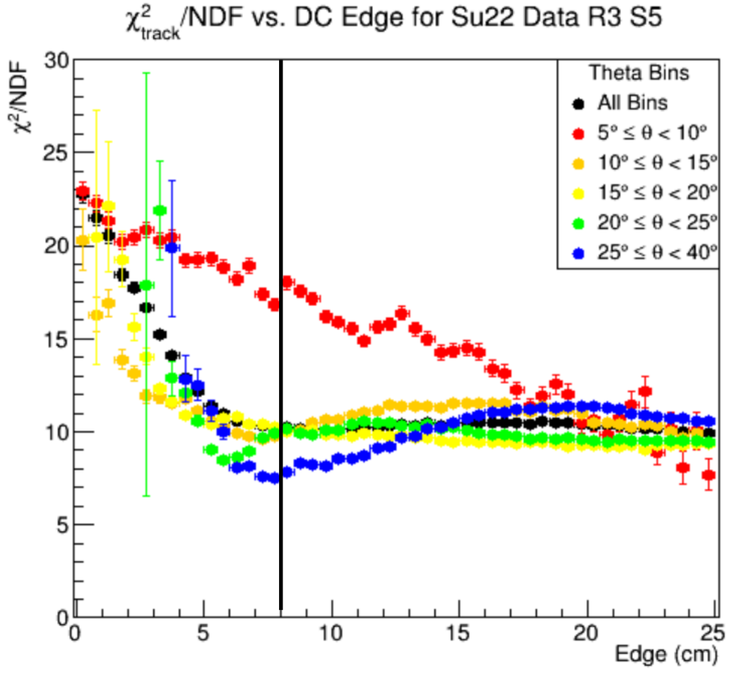

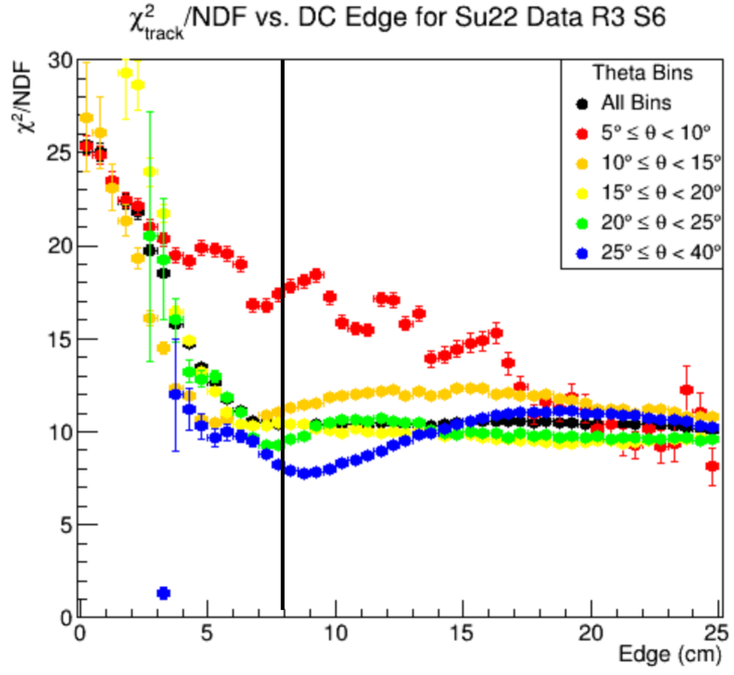

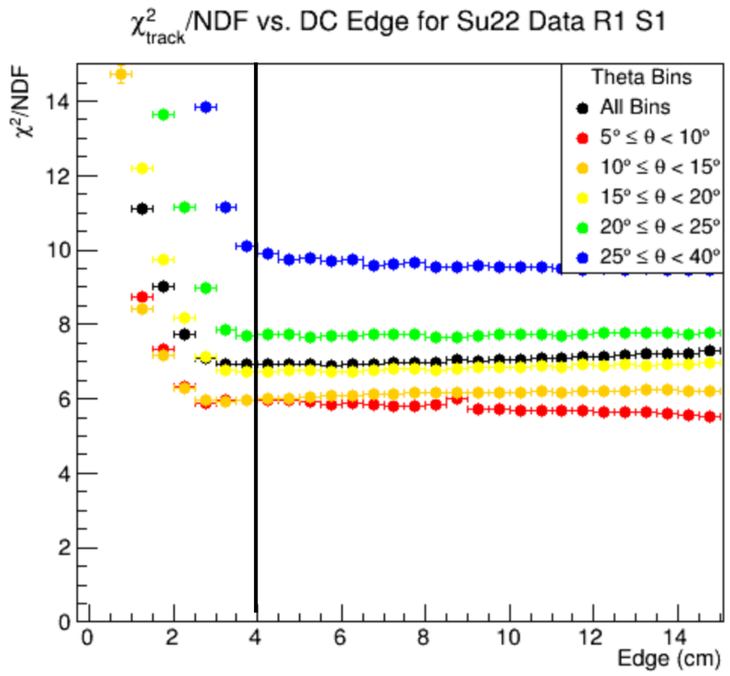

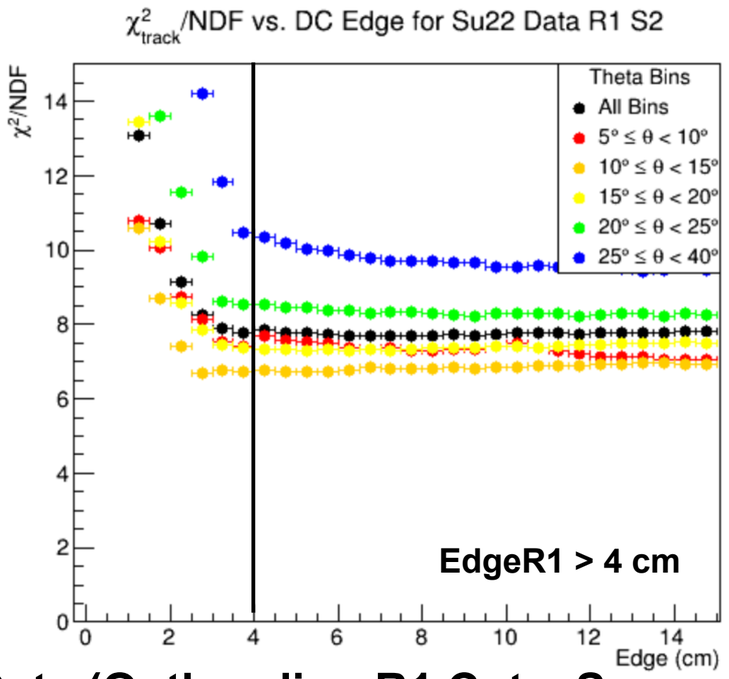

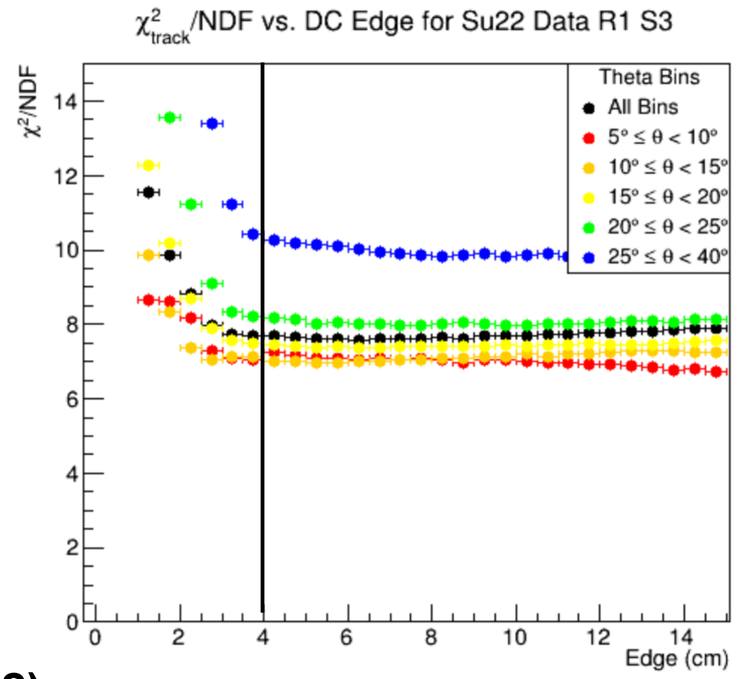

π^+ Data (Outbending R1 Cuts, Summer 2022)

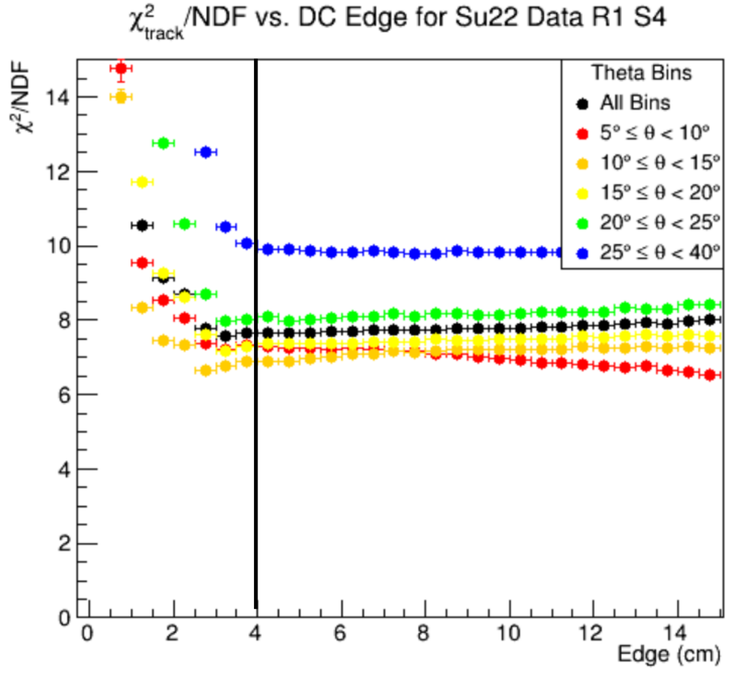

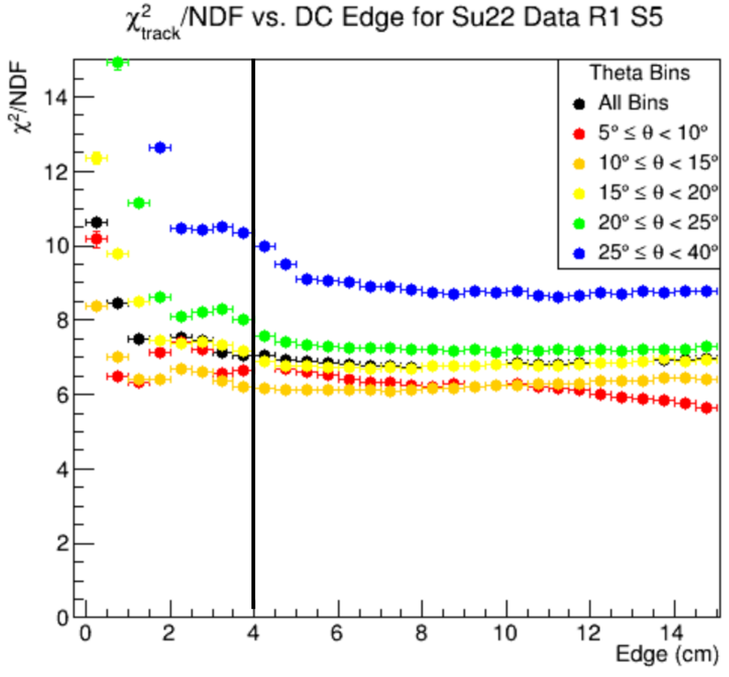

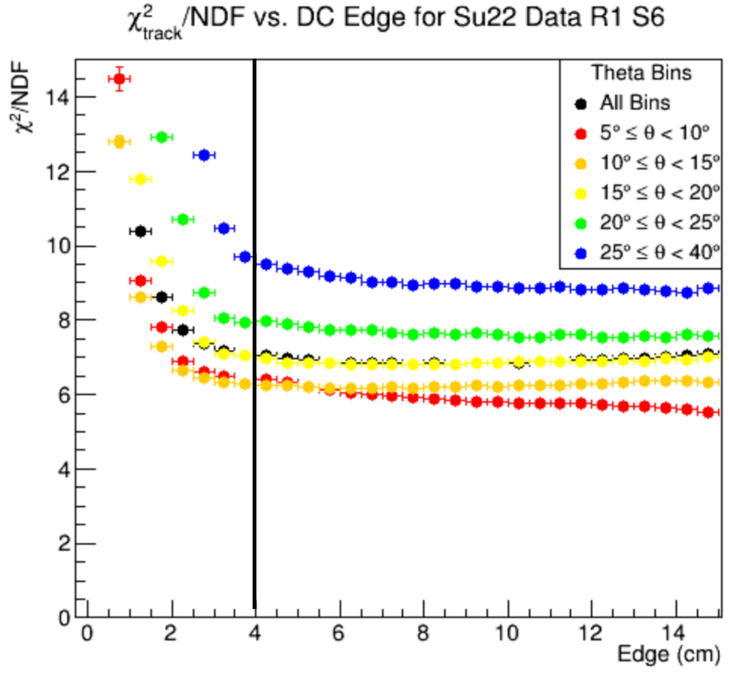

Faraday Cup Charge Asymmetry

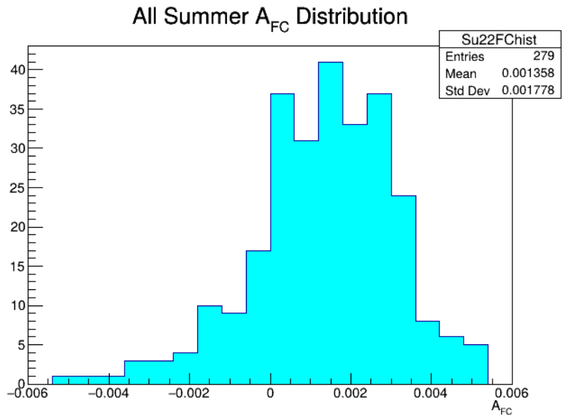

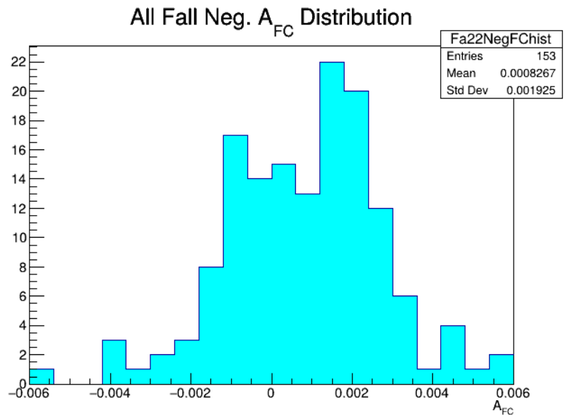

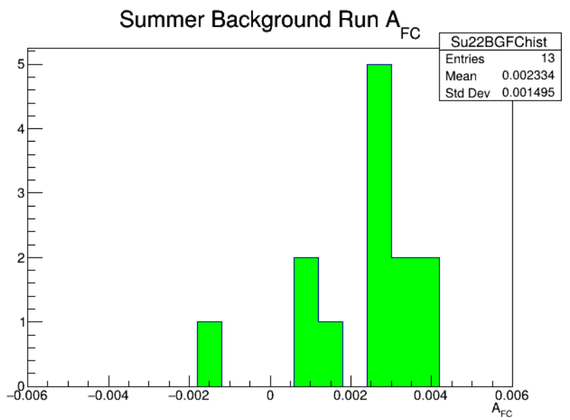

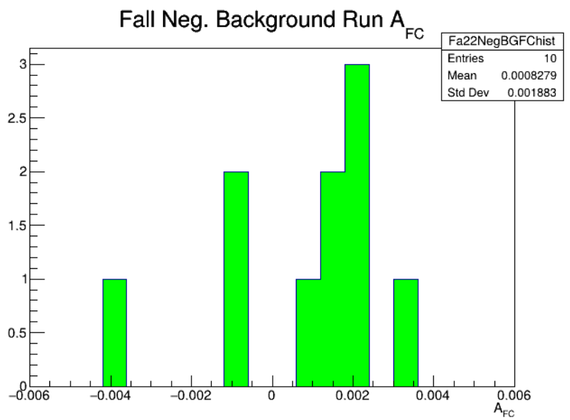

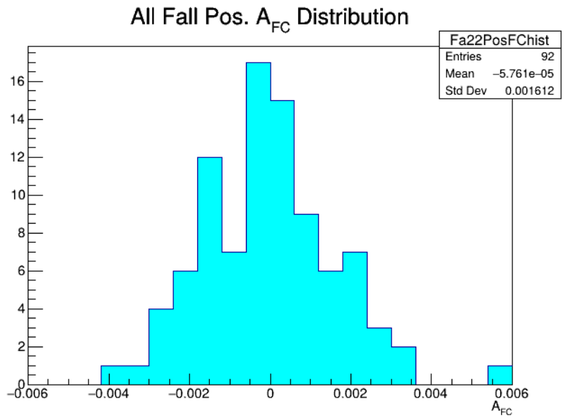

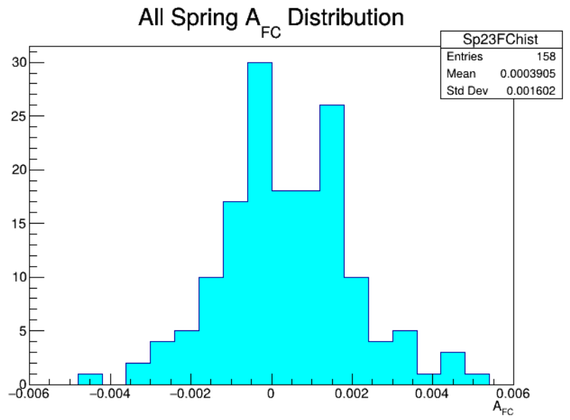

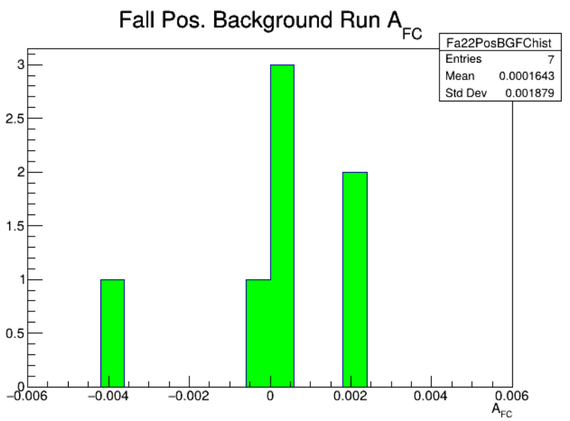

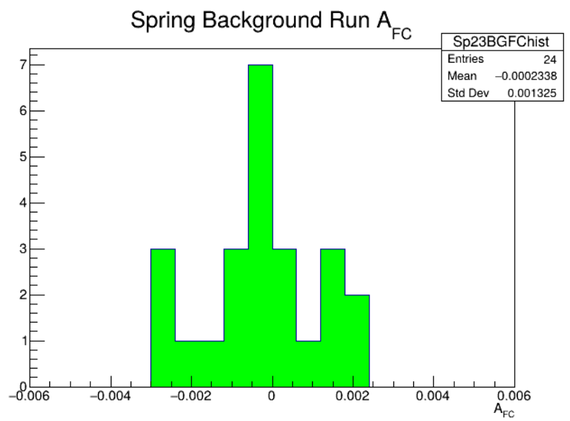

- Histograms of the FC charge asymmetries for each run period, looking at all polarized and unpolarized targets
- There's a notable asymmetry for the summer data and a slight asymmetry for the fall negative solenoid period
- The fall positive solenoid and spring inbending periods were mostly consistent with zero

- Histograms of the FC charge asymmetries for each run period, looking at the unpolarized targets only (carbon, CH2, CD2, empty, foils)

$$A_{LU} = \frac{N^+ - N^-}{N^+ + N^-}$$

$N^{\pm}$ = raw counts for the $\pm$ helicity state

$$A_{FC} = \frac{FC^+ - FC^-}{FC^+ + FC^-}$$

$FC^{\pm}$ = Faraday Cup charge for the $\pm$ helicity state

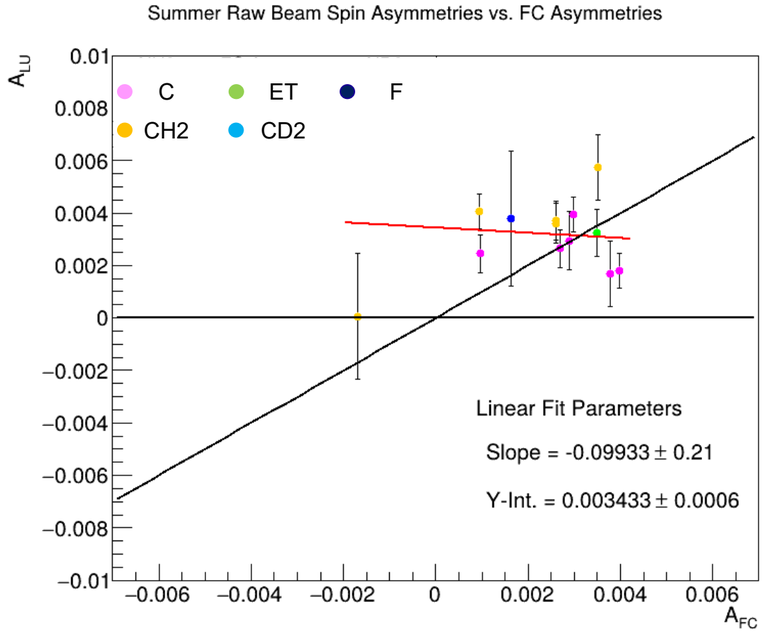

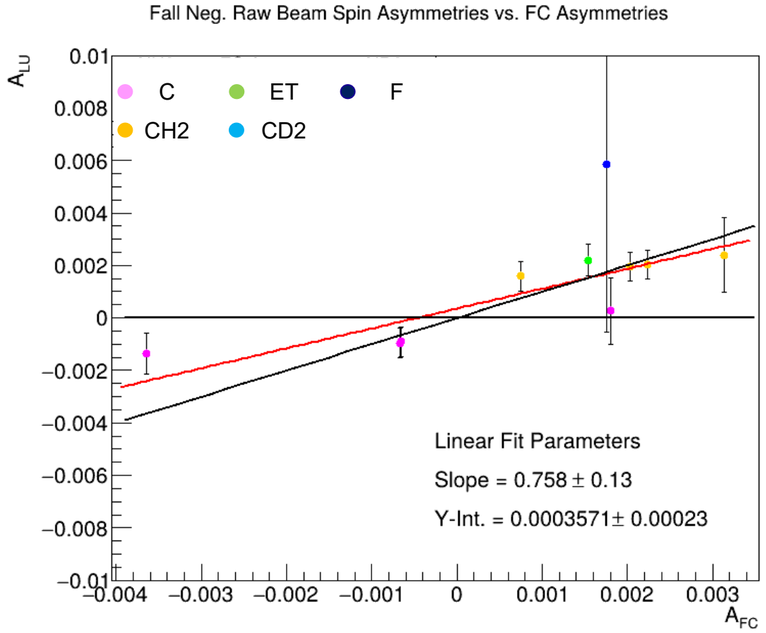

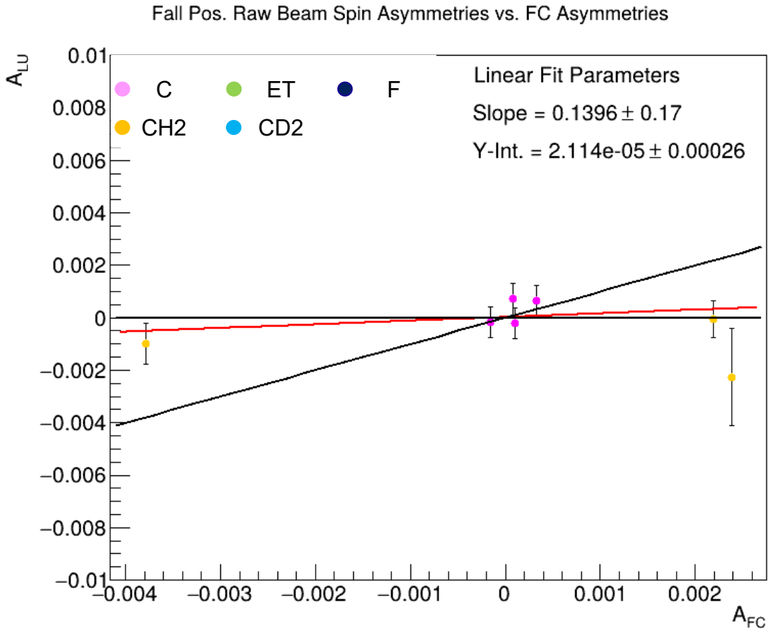

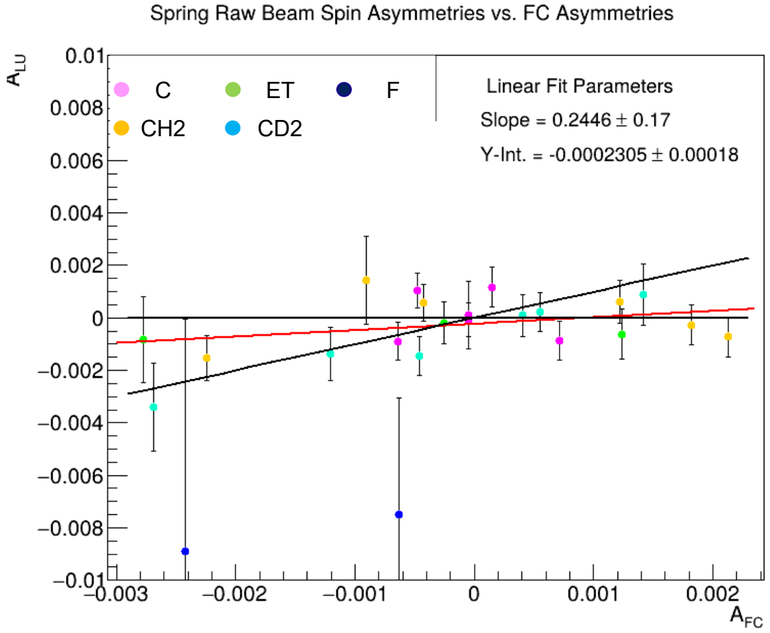

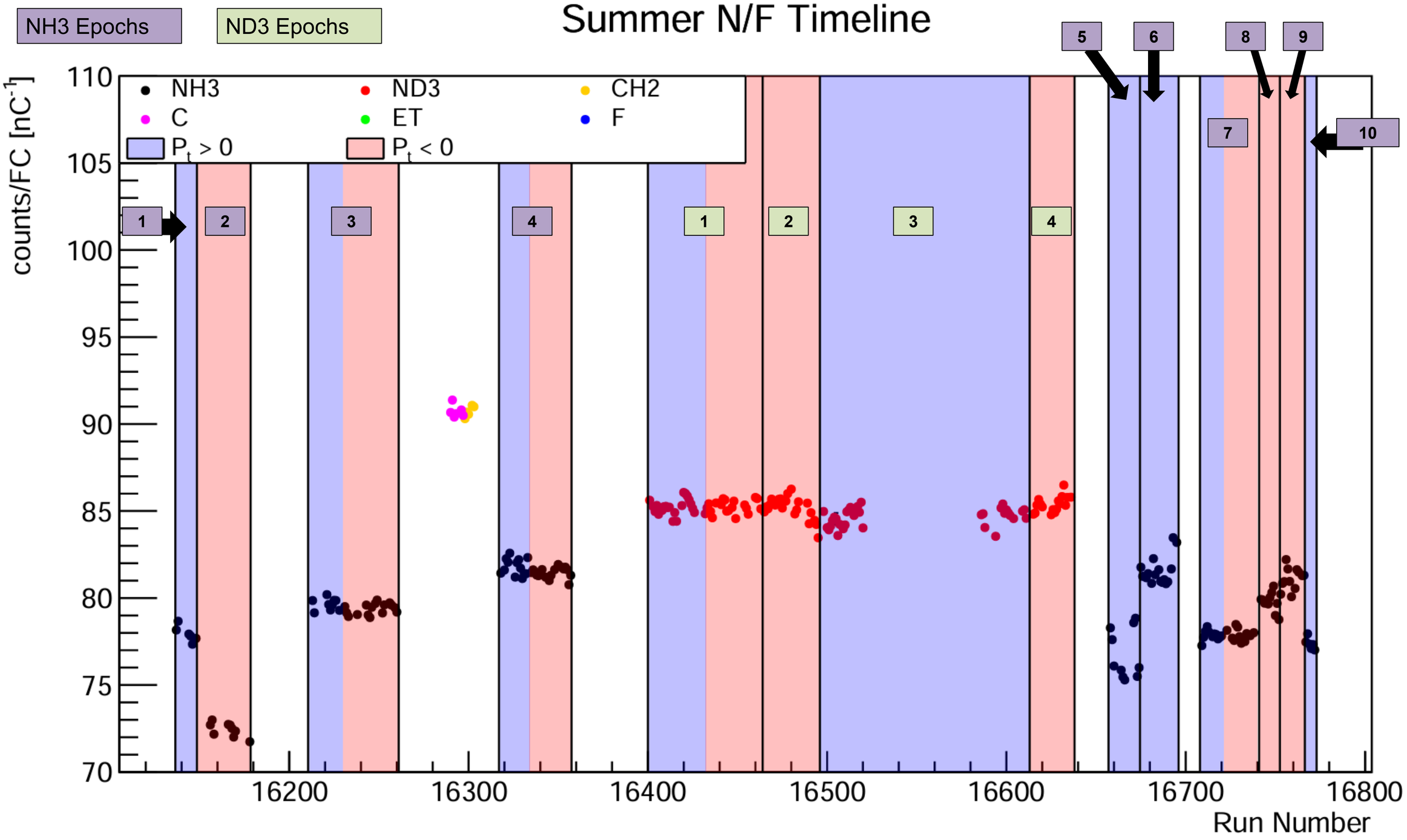
NH3 Epochs
ND3 Epochs
Summer N/F Timeline
NH3
ND3
CH2
C
ET
F
$P_t > 0$
$P_t < 0$
counts/FC [nC^{-1}]
Run Number
1
2
3
4
5
6
7
8
9
10
110
105
100
95
90
85
80
75
70
16200
16300
16400
16500
16600
16700
16800

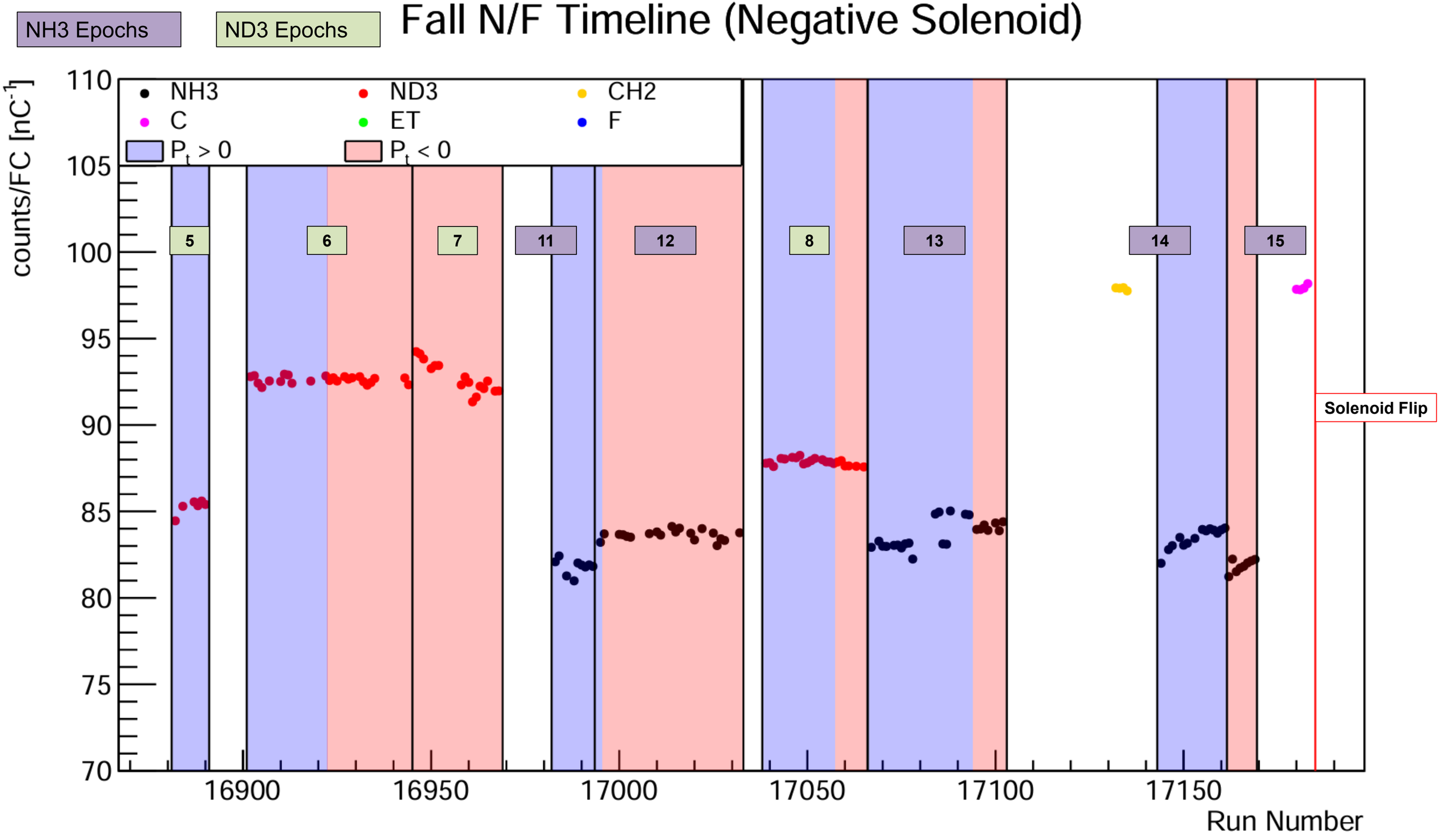
NH3 Epochs
ND3 Epochs
Fall N/F Timeline (Negative Solenoid)
counts/FC [nC^{-1}]
NH3
ND3
CH2
C
ET
F
$P_t > 0$
$P_t < 0$
5
6
7
11
12
8
13
14
15
Solenoid Flip
110
105
100
95
90
85
80
75
70
16900
16950
17000
17050
17100
17150
Run Number

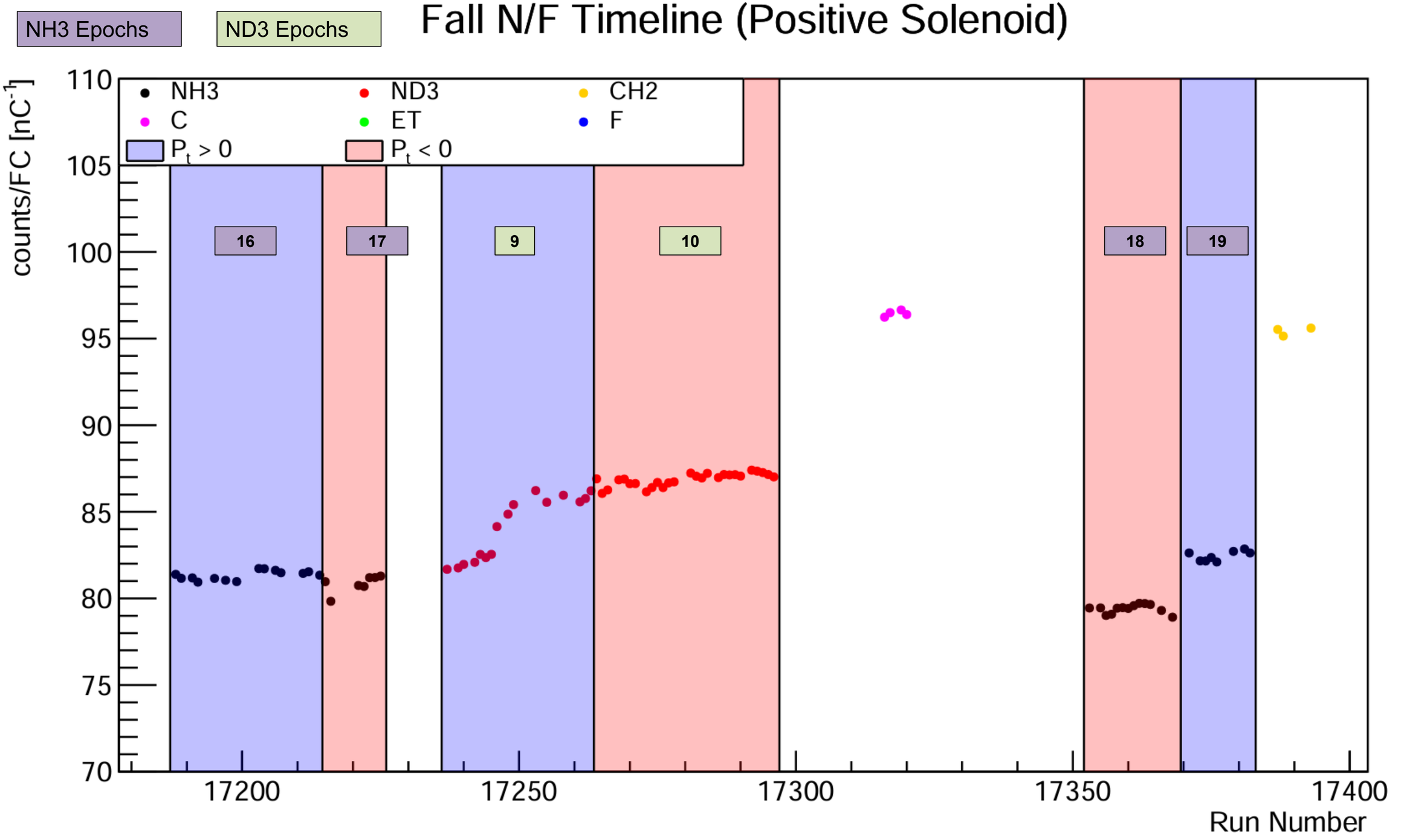
NH3 Epochs
ND3 Epochs
Fall N/F Timeline (Positive Solenoid)
NH3
ND3
CH2
C
ET
F
$P_t > 0$
$P_t < 0$
16
17
9
10
18
19
counts/FC [nC^{-1}]
110
105
100
95
90
85
80
75
70
17200
17250
17300
17350
17400
Run Number

NH3 Epochs

ND3 Epochs

Spring N/F Timeline (Inbending)

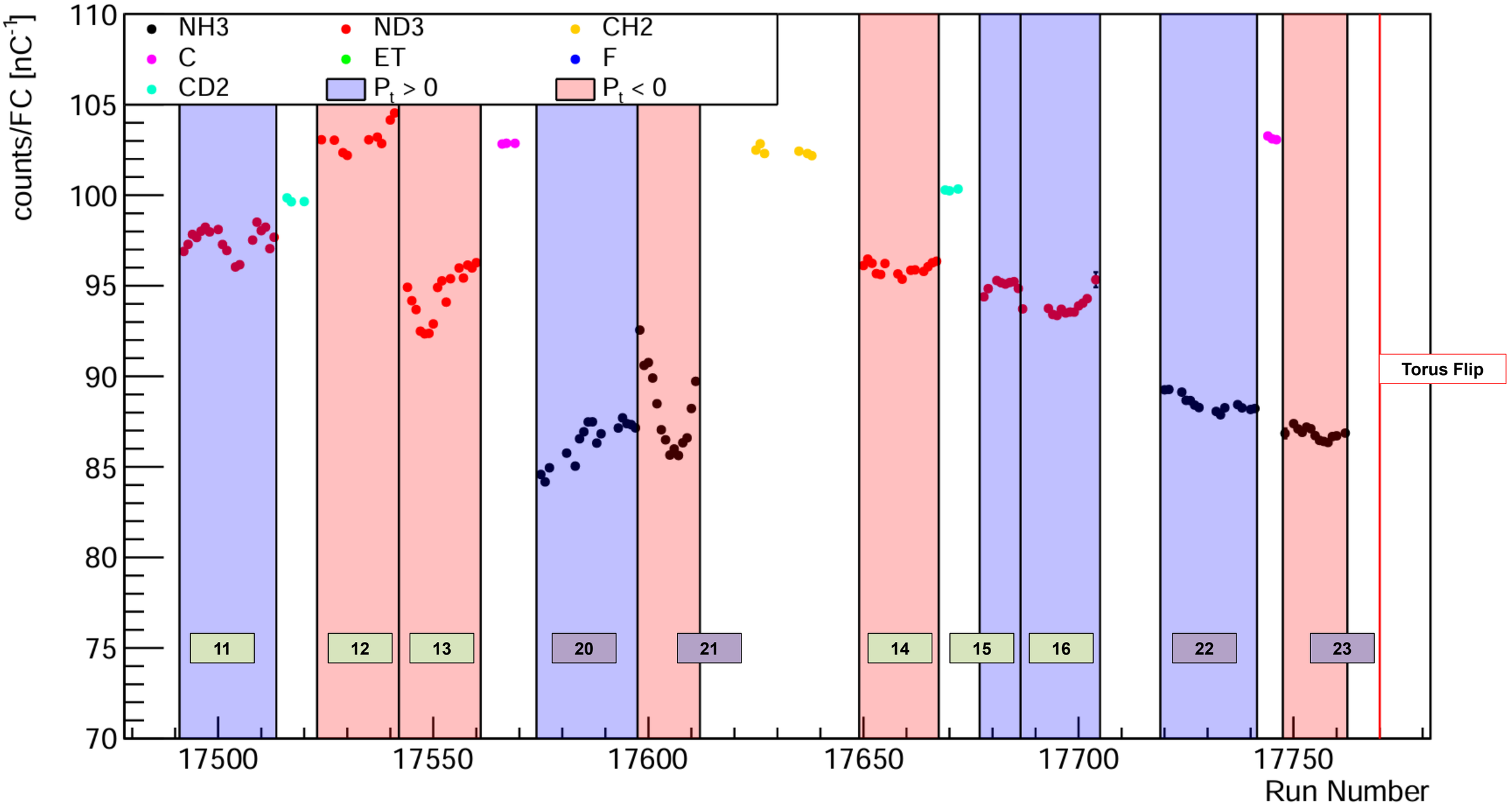

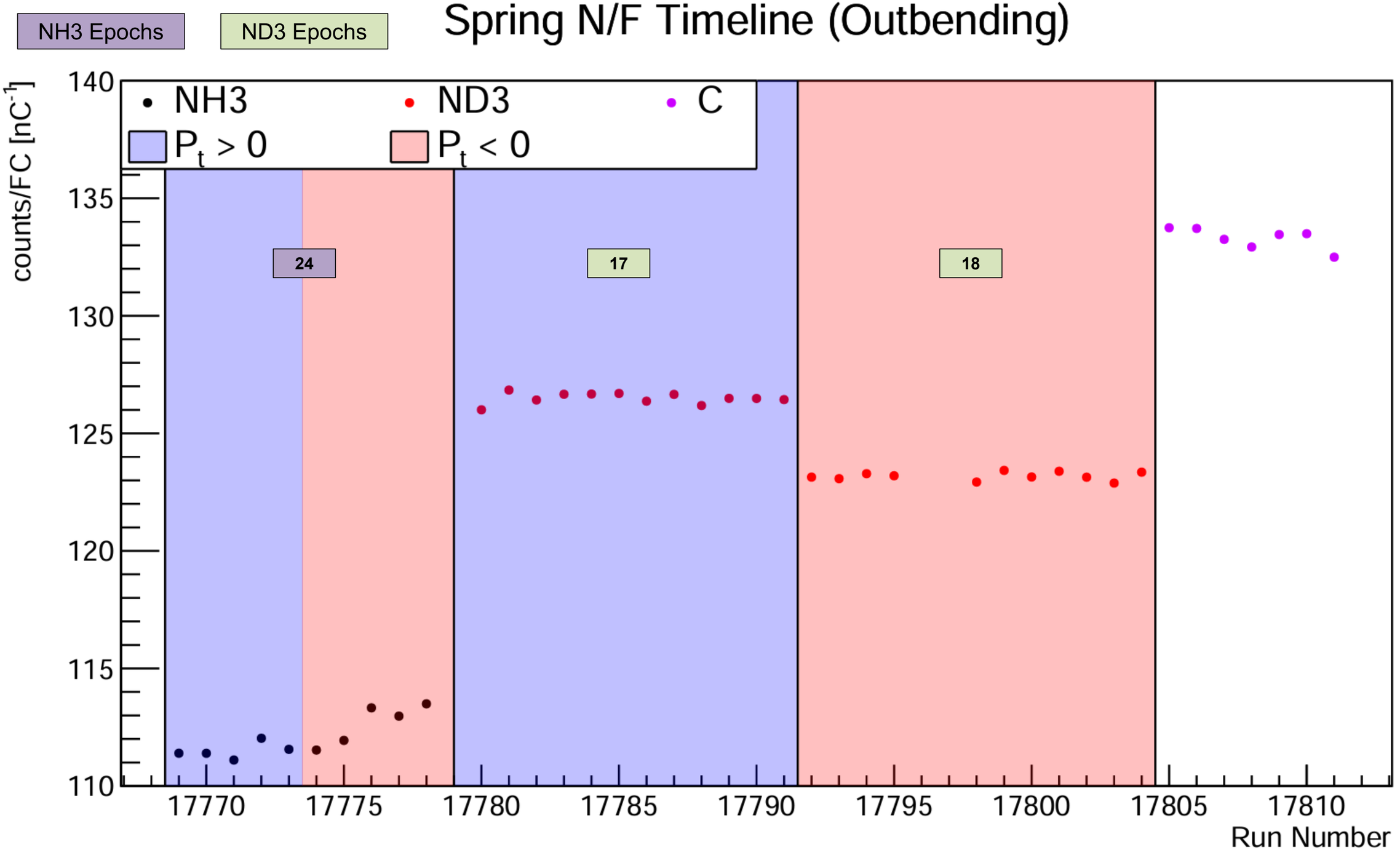
NH3 Epochs
ND3 Epochs
Spring N/F Timeline (Outbending)
NH3
ND3
C
$P_t > 0$
$P_t < 0$
24
17
18
counts/FC [nC^{-1}]
140
135
130
125
120
115
110
17770
17775
17780
17785
17790
17795
17800
17805
17810
Run Number

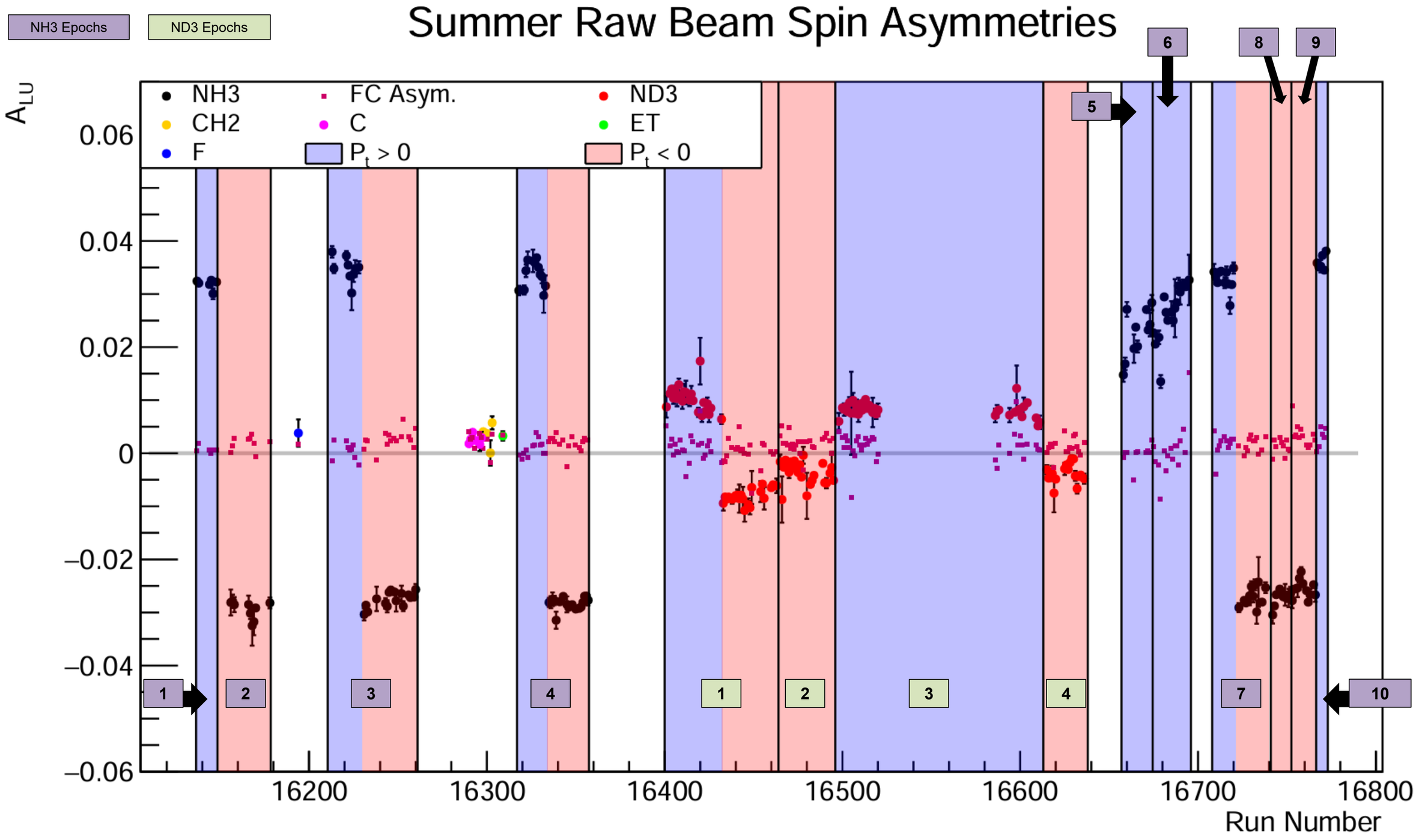
NH3 Epochs
ND3 Epochs
Summer Raw Beam Spin Asymmetries
NH3
CH2
F
FC Asym.
C
$P_t > 0$
ND3
ET
$P_t < 0$
A_{LU}
0.06
0.04
0.02
0
−0.02
−0.04
−0.06
16200
16300
16400
16500
16600
16700
16800
Run Number
1
2
3
4
1
2
3
4
5
6
7
8
9
10

NH3 Epochs

ND3 Epochs

Fall Raw Beam Spin Asymmetries (Negative Solenoid)

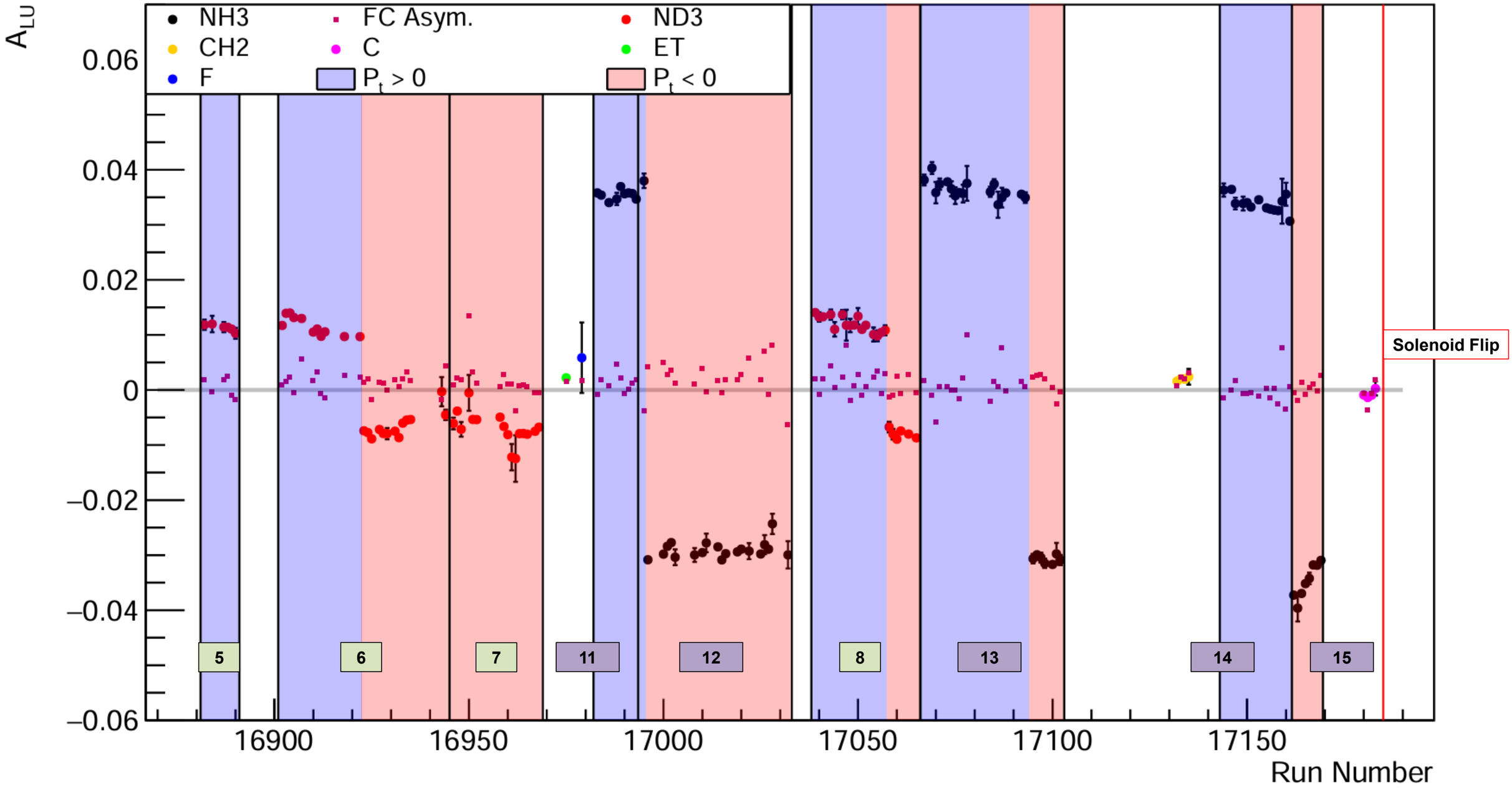

NH3 Epochs

ND3 Epochs

Fall Raw Beam Spin Asymmetries (Positive Solenoid)

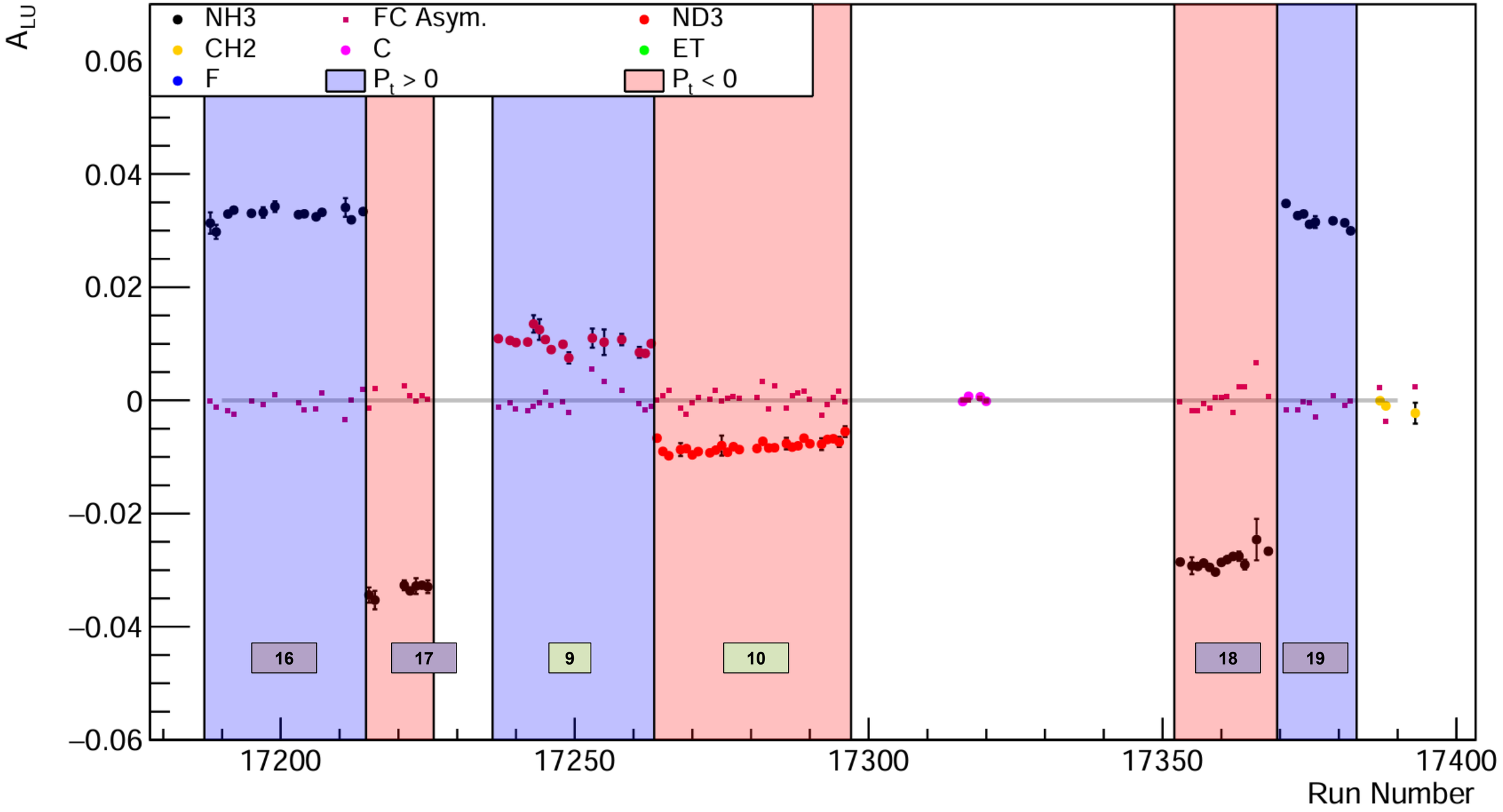

NH3 Epochs

ND3 Epochs

Spring Raw Beam Spin Asymmetries (Inbending)

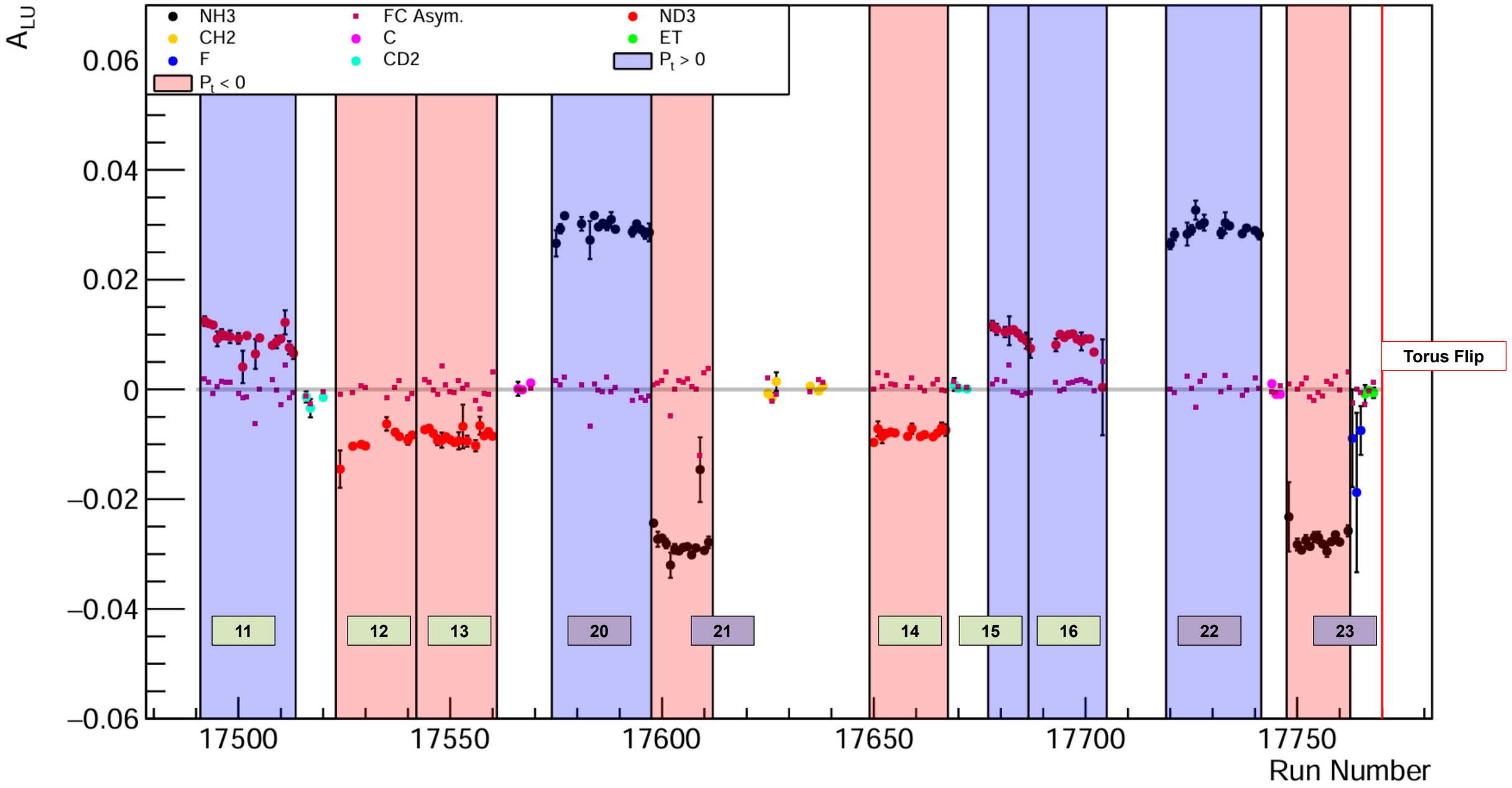

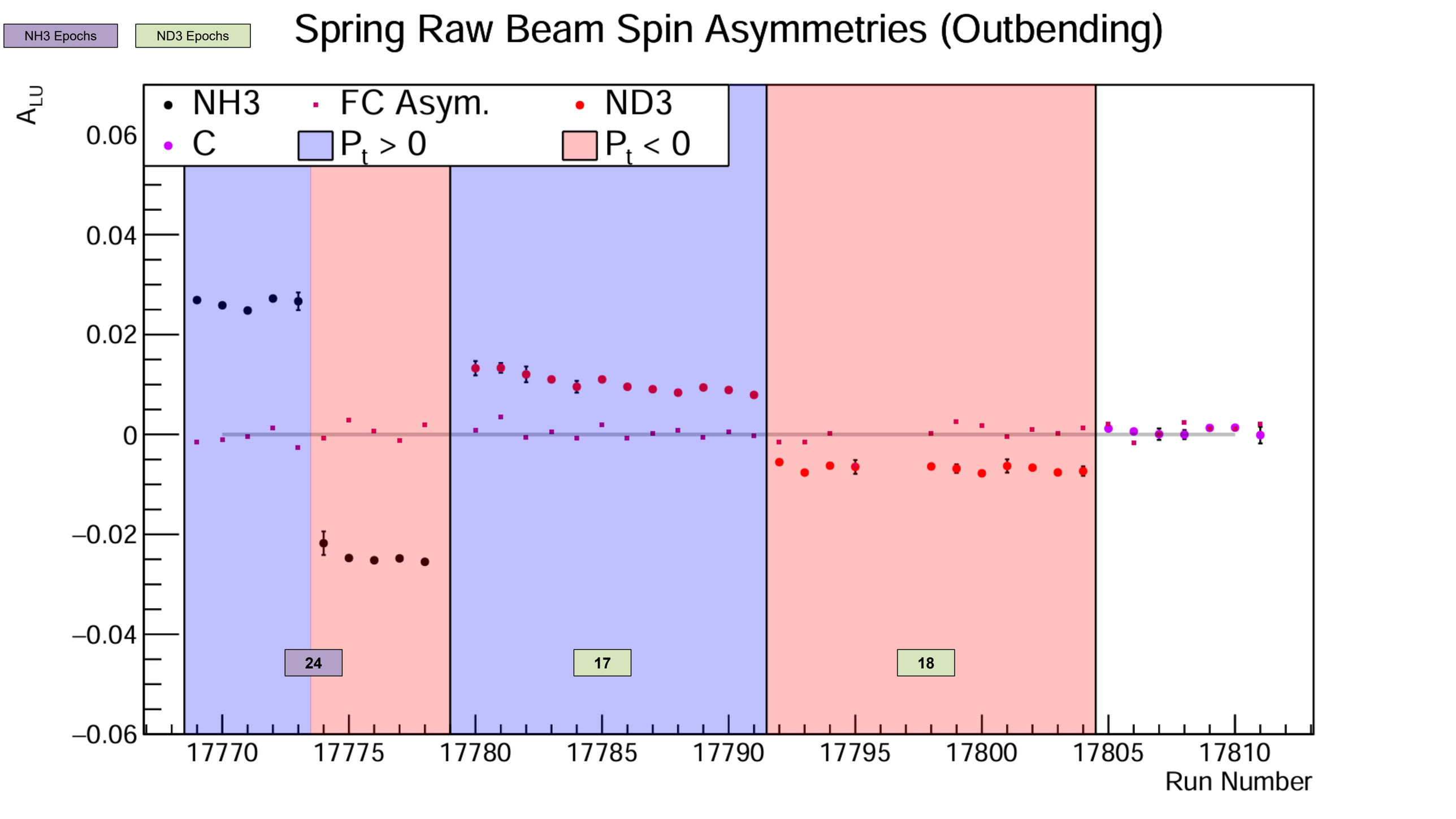
NH3 Epochs
ND3 Epochs
Spring Raw Beam Spin Asymmetries (Outbending)
NH3
FC Asym.
ND3
C
$P_t > 0$
$P_t < 0$
A_{LU}
0.06
0.04
0.02
0
−0.02
−0.04
−0.06
24
17
18
17770
17775
17780
17785
17790
17795
17800
17805
17810
Run Number